Provenance of the Campanian-Maastrichtian Sandstone, Northern Bida Basin: Evidence from Facies Analysis, Detrital Zircon Morphology and Whole-Rock Geochemistry

Adepoju, S.A., [1*], Ojo, O.J.[2], Akande, S.O.[3] and Sreenivas, B.[4]

[1]Department of Geology and Mineral Sciences, Kwara State University, Malete, Kwara State
[2]Department of Geology, Federal University Oye Ekiti
[3]Department of Geology and Mineral Sciences, University of Ilorin
[4]Council of Scientific and Industrial Research–National Geophysical Research Institute, Hyderabad 500007, India

ABSTRACT

The sediments in the northern Bida Basin, Nigeria were investigated on the basis of facies analysis, architectural elements, sandbody geometry and paleocurrents, whole-rock geochemical and zircon cathodoluminescent studies. The aim was to interprete the depositional environments and provenance as well as a platform for further reservoir characterization. Regional distribution, architecture and morphology of the sandstone were interpreted through the identification of ten distinctive sub-facies that were classified within four facies associations; intraformational conglomerate, braided fluvial channels, meandering channels and fluvial overbank/floodplain. Six identified architectural elements within the study area; channels (CH), gravelbars and bedforms (GB), lateral accretion (LA), laminated sand sheet (LS), sandy bedforms (SB) and overbank fines (OF) showed a river system settings ranging from floodplains to more high energy, braided fluvial systems of low sinuosity. Sheet and blanket Sandbody geometry that characterizes sandstone reservoir heterogeneity by their vertical and lateral connectivity of sand bodies are common in the central and northern part while wedge and lobate types are common in the southern and eastern parts. Paleocurrent data obtained indicate dominant influence of southwestern and minor southeastern paleocurrent transport directions across basin axis. Detrital zircon morphological studies reveal changes in the primary sources during depositional history; prismatic and lamellar detrital zircon types with a well-developed oscillatory zoning typical of magmatic crystallization were observed in Bida Formation whereas distinct populations of short and acicular types in Enagi Formation characterizes preservation of crustal rocks. The geochemical proxies; Al_2O_3/TiO_2, SiO_2/Al_2O_3, K_2O/Al_2O_3, La/Th, La/Co, Th/Co, La/Sc, Cr/Th, Zr/Nb and Zr/Th with chondrite-normalized REE patterns, light REE enrichment, heavy REE flat pattern and negative Eu anomalies revealed sediments' derivation mainly from felsic source rocks. A higher Zr/Sc and Zr/Hf ratio with Th/Sc and Zr/Sc binary plot reflects considerable zircon enrichment in the source areas. Discrimination plots; log(K_2O/Na_2O) versus SiO_2, TiO_2 versus (Fe_2O_3+MgO), Al_2O_3/SiO_2 versus (Fe_2O_3+MgO) and $SiO_2/20$-(K_2O+Na_2O)-(TiO_2+Fe_2O_3+MgO), La/Y versus Sc/Cr, La-Th-Sc, Th-Sc-Zr/10 indicate passive continental margin paleotectonic settings. In conclusion, this integrated study revealed that fluvial sediment input in the northern Bida Basin Nigeria is sourced from Precambrian Basement Complex with possible mixing from two igneous source materials.

Keywords: Sedimentology, Sandstone, Facies, Paleoenvironment, Geochemistry, Zircon, Provenance Bida Basin.

INTRODUCTION

The study area is located in parts of northern Bida Basin, north-central Nigeria. The Bida Basin which is one of the hinterland sedimentary basins in Nigeria is northwest-southeast trending intracratonic structural depression and contiguously adjacent with Sokoto and Anambra Basins in the north-west and south-east respectively (Figure 1). The basin which is geographically sub-divided into the northern and southern parts to accommodate the fast and wide facies changes across its long and large areal extent (Braide, 1992) has a sedimentary fill of about 4km (Ojo, 1984; Udensi and Osasuwa, 2004). Several authors including King (1950) and Kennedy (1965) have worked on the evolution of Bida Basin and described it as a rift bounded tensional structure produced by faulting associated with the Benue Trough System (BTS) and drifting apart of South America and Africa plates. Kogbe *et al.,* (1981), and Ojo and Ajakaiye (1989) concluded from their independent geophysical research work and

© Copyright 2020. Nigerian Association of Petroleum Explorationists.
All rights reserved.

The first author thanks the Department of Science and Technology, Government of India for the CV Raman Fellowship for African Researchers (2016). Member of the Isotope Geochemistry and Geochronology group are also appreciated for hospitality and support during the six months Research Visitation at of the CSIR-NGRI. Dr. Vijaya Kumar, Ms. Manju and Mr. E.G.H.N. Santhos are also appreciated for help during CL analyses and Mr. Balu Gugulothu for support during geochemical analyses.

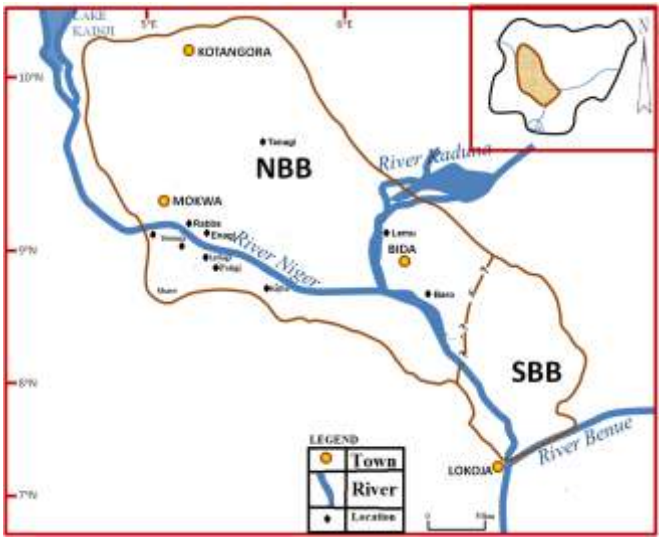


Figure 1: Map of the study area showing study location and important towns and the inset map of Nigeria showing the position of Bida Basin (Inset).

Table 1: Regional stratigraphic successions in the Bida Basin modified after Ojo and Akande (2012).

PERIOD	AGE	NORTHERN BIDA SUB-BASIN	SOUTHERN BIDA SUB-BASIN	LITHOLOGY
CRETACEOUS	MAASTRICHTIAN	Batati Formation	Agbaja Formation	
		Enagi Formation		
		Sakpe Formation	Patti Formation	
	CAMPANIAN	Bida Formation: Jima member	Lokoja Formation	
		Bida Formation: Doko member		
PRECAMBRIAN	LOWER PROTEROZOIC	Basement Complex		

Table 2: Lithofacies and sub-facies types in the study area.

Lithofacies	Sub-facies Code (after Miall, 1985, 1988, 1992)	Description	Location
Conglomerate	Clast Supported Conglomerate (Gcm)	Massive, poorly sorted, clast-supported, imbricated conglomerate.	Patigi and Baganko
	Matrix Supported Conglomerate (Gmm)	Massive, poorly sorted, subrounded to subangular conglomerate.	Patigi, Baganko, Gbale, Share and Baro
	Crudely bedded Conglomerate (Gh)	Weakly laminated, poorly sorted, very coarse-pebbly sandstone.	Shonga, Gbale, Gbugbu, Lafiagi, Baganko and Baro
Sandstone	Crudely bedded Sandstone (Se)	Weakly bedded sandstone (fine to very coarse grained).	Share, Shonga, Rabba, Bida, Enagi, Baro, Lemu and Doko
	Planar cross-bedded sandstone (Sp)	Planar cross bedded sandstone (fine to very coarse grained).	Kutigi, Doko, Bida, Tanagi and Rabba
	Rippled cross-bedded sandstone (Sr)	Rippled cross-bedded sandstone (fine to very coarse grained).	Share and Rabba
	Horizontally stratified sandstone (Sh)	Planar laminated sandstone (fine to very coarse grained).	Rabba, Bida, Kutigi, Tanagi, Lemu and Doko
	Massive sandstone (Sm)	Massive sandstone (fine to very coarse grained).	Share, Shonga, Doko, Enagi, Lemu, Lafiagi and Rabba
Mudstone	Finely laminated mudstone (siltstone and claystone) (Fl)	Planar laminated claystone to siltstone.	Share, Kutigi, Enagi, Rabba, and Tanagi
	Massive mudstone (siltstone and claystone) (Fm)	Massive claystone to siltstone.	Share, Gbugbu, Kutigi, Enagi, Rabba and Tanagi

Table 3: Paleocurrent data of planar- cross lamination/bedding and clast imbrication and their locations within the study area.

Locality	Maraba		Rafingora		Manigi		Rabba		Enagi		Doko		Jima		Patigi (Pebble)	
	Azimuth	Dip	Azimuth	Dip	Azimuth	Dip	Azimuth	Dip	Azimuth	Dip	Azimuth	Dip	Azimuth	Dip	Azimuth	Azimuth
1	060	40°E	029	48°E	040	40°E	086	20°E	080	20°E	270	10°W	220	18°E	020°	010°
2	058	60°E	032	50°E	044	50°E	090	18°E	080	26°E	280	8°W	200	20°E	005°	020°
3	061	40°E	030	50°E	040	54°E	090	20°E	080	18°E	270	12°W	320	10°E	002°	010°
4	060	46°E	032	52°E	040	52°E	090	22°E	082	22°E	280	12°W	210	18°E	009°	004°
5	062	44°E	031	46°E	039	48°E	090	18°E	079	20°E	270	8°W	220	16°E	020°	012°
6	060	44°E	033	48°E	041	48°E	040	40°E	078	18°E	280	14°W	220	18°E	002°	352°
7	062	44°E	032	50°E	040	50°E	080	16°E	080	20°E	270	12°W	200	18°E	020°	340°
8	060	40°E	032	48°E	040	48°E	089	20°E	080	22°E	320	10°W	220	20°E	003°	020°
9							090	18°E	080	18°E	270	8°W	218	22°E	006°	014°
10							089	28°E	080	22°E	280	12°W	216	22°E	007°	010°

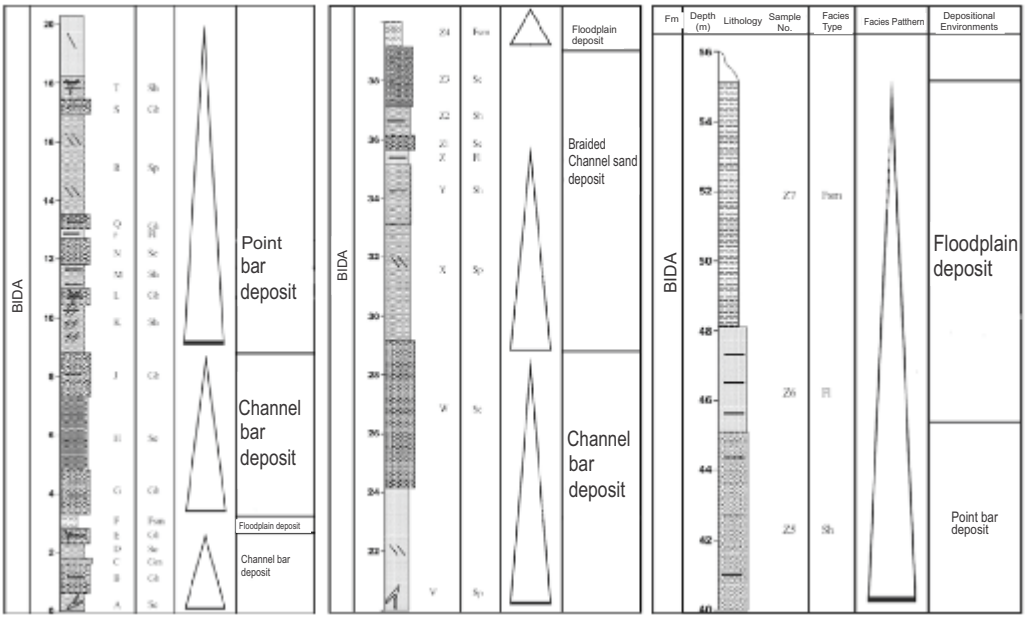


Figure 2a: Lithological section of Bida Formation exposed at Doko (DOK-1); Longitude: 005°37.545'E; Latitude: 08°56.744'N.

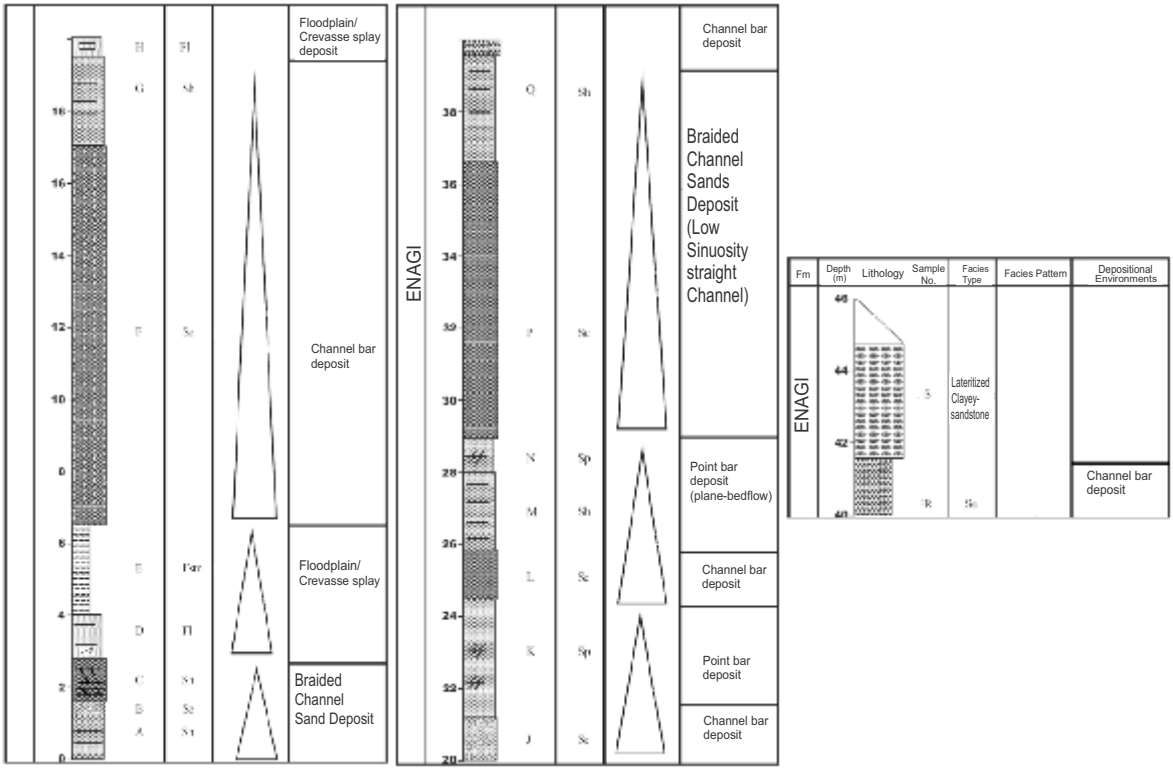


Figure 2b: Lithological section of Enagi Formation at exposed Agbonna Ridge (AGB-1); Longitude: 004°58'36.3"E; Latitude: 08°49'32.3"N.

Table 4a: Major Element Composition (%) of sandstone in Northern Bida Basin

Formation	Location	Sample No	SiO_2	Al_2O_3	Fe_2O_3	MnO	MgO	CaO	Na_2O	K_2O	TiO_2	P_2O_5	Al_2O_3/TiO_2	SiO_2/Al_2O_3	K_2O/Al_2O_3
Enagi	**Agbonna**	AGB-1B	88.50	7.84	1.67	0.00	0.02	0.05	0.04	0.12	0.33	0.04	23.76	11.29	0.02
	Agbonna	AGB-1K	79.89	13.02	4.18	0.02	0.05	0.05	0.03	0.05	1.00	0.12	13.02	6.14	0.00
	Agbonna	AGB-1G	82.09	14.71	1.59	0.01	0.05	0.01	0.08	0.50	1.41	0.06	10.43	5.58	0.03
	Agbonna	AGB-1D	74.98	18.38	3.82	0.01	0.07	0.05	0.07	0.24	1.22	0.07	15.07	4.08	0.01
	Enagi	ENG-1B	84.56	9.40	1.89	0.01	0.06	0.16	0.22	1.31	0.57	0.02	16.49	9.00	0.14
	Enagi	ENG-1E	89.63	7.14	1.48	0.00	0.02	0.03	0.08	0.97	0.25	0.02	28.56	12.55	0.14
	Enagi	ENG-1J	90.88	4.74	1.83	0.01	0.00	0.01	0.07	0.85	0.17	0.02	27.88	19.17	0.18
	Enagi	ENG-1L	84.98	9.51	4.18	0.01	0.05	0.05	0.08	0.88	0.40	0.02	23.78	8.94	0.09
	Enagi	ENG-1N	86.26	7.13	4.52	0.01	0.02	0.02	0.06	0.66	0.47	0.02	15.17	12.10	0.09
	Enagi	ENG-1V	92.44	6.07	1.21	0.01	0.01	0.04	0.03	0.14	0.75	0.02	8.09	15.23	0.02
	Kudu	KUD-1A	83.41	7.95	2.57	0.01	0.05	0.03	0.01	0.08	1.34	0.02	5.93	10.49	0.01
	Kudu	KUD-1B	74.98	10.10	7.56	0.01	0.06	0.03	0.01	0.09	1.35	0.07	7.48	7.42	0.01
	Kudu	KUD-1C	87.93	7.46	0.89	0.01	0.04	0.04	0.01	0.05	1.00	0.02	7.46	11.79	0.01
	Kudu	KUD-1F	82.39	7.45	4.73	0.01	0.06	0.02	0.01	0.06	1.53	0.03	4.87	11.06	0.01
	Kutigi	KUT-3a	90.93	4.15	2.01	0.01	0.02	0.03	0.01	0.04	0.37	0.04	11.22	21.91	0.01
	Kutigi	KUT-2D	90.86	4.82	1.03	0.01	0.01	0.01	0.01	0.04	0.23	0.02	20.96	18.85	0.01
	Kutigi	KUT-2G	89.59	4.35	2.06	0.01	0.03	0.02	0.01	0.04	0.35	0.02	12.43	20.60	0.01
	Kutigi	KUT-2K	89.60	4.35	1.58	0.01	0.04	0.04	0.01	0.04	0.51	0.02	8.53	20.60	0.01
	Shonga	SHG-1B	89.99	4.95	1.69	0.01	0.00	0.01	0.02	0.00	0.16	0.01	30.94	18.18	0.00
	Shonga	SHG-1K	88.52	7.15	1.32	0.02	0.00	0.01	0.02	0.00	1.02	0.01	7.01	12.38	0.00
	Shonga	SHG-1P	89.15	5.73	1.21	0.01	0.00	0.00	0.02	0.00	0.63	0.01	9.10	15.56	0.00
	Tanagi	TAN-1A	90.19	3.49	3.90	0.01	0.00	0.01	0.01	0.00	0.11	0.02	31.73	25.84	0.00
	Tanagi	TAN-1C	77.48	13.97	5.62	0.01	0.04	0.04	0.04	0.65	0.43	0.02	32.49	5.55	0.05
Bida	**Bida**	BDA-1A	84.68	11.25	1.84	0.00	0.01	0.01	0.02	0.01	0.23	0.02	48.91	7.53	0.00
	Bida	BDA-1B	88.54	8.37	1.37	0.01	0.01	0.01	0.02	0.02	0.32	0.02	26.16	10.58	0.00
	Bida	BDA-1D	89.22	4.59	1.52	0.01	0.00	0.02	0.02	0.01	0.28	0.01	16.39	19.44	0.00
	Bida	BDA-1K	86.04	6.32	3.17	0.04	0.02	0.02	0.02	0.01	4.89	0.04	1.29	13.61	0.00
	Bida	BDA-1R	87.55	8.12	2.28	0.01	0.01	0.01	0.02	0.01	0.40	0.02	20.30	10.78	0.00
	Doko	DOK-1D	78.74	14.25	4.21	0.01	0.04	0.02	0.02	0.03	0.92	0.03	15.49	5.53	0.00
	Doko	DOK-1F	80.04	14.52	2.06	0.01	0.02	0.03	0.02	0.03	0.28	0.03	51.86	5.51	0.00
	Doko	DOK-1K	84.36	10.47	2.56	0.01	0.01	0.02	0.02	0.01	0.30	0.03	34.90	8.06	0.00
	Doko	DOK-1T	86.21	9.39	2.62	0.01	0.00	0.01	0.01	0.00	0.30	0.03	31.30	9.18	0.00
	Doko	DOK-1X	87.91	9.24	0.67	0.00	0.01	0.01	0.02	0.01	0.30	0.03	30.80	9.51	0.00
	Gbale	GBL-1A	74.56	12.08	2.97	0.01	0.20	0.11	0.11	2.90	0.27	0.01	44.74	6.17	0.24
	Gbale	GBL-1C	84.44	8.90	1.28	0.01	0.02	0.01	0.02	0.77	0.25	0.01	35.60	9.49	0.09
	Gbale	GBL-1D	84.25	7.83	2.44	0.01	0.03	0.02	0.01	0.14	0.58	0.01	13.50	10.76	0.02
	Gbale	GBL-1E	79.44	9.06	2.31	0.01	0.39	0.21	0.12	3.24	0.18	0.01	50.33	8.77	0.36
	Gbugbu	GBU-1A	74.51	13.36	2.99	0.01	0.06	0.01	0.04	1.40	0.32	0.01	41.75	5.58	0.10
	Gbugbu	GBU-1B	87.07	6.36	1.15	0.01	0.07	0.01	0.06	1.61	0.28	0.01	22.71	13.69	0.25
	Gbugbu	GBU-1D	90.59	4.65	0.76	0.01	0.02	0.01	0.06	1.61	0.18	0.01	25.83	19.48	0.35
	Gbugbu	GBU-1D	90.59	4.65	0.76	0.01	0.02	0.01	0.06	1.61	0.18	0.01	25.83	19.48	0.35
	Patigi	PTG-1A	88.25	4.52	1.75	0.01	0.05	0.01	0.04	1.31	0.19	0.01	23.79	19.52	0.29
	Patigi	PTG-1B	87.08	4.98	4.03	0.01	0.04	0.01	0.01	0.26	0.27	0.01	18.44	17.49	0.05
	Patigi	PTG-1D	68.69	7.04	17.57	0.02	0.05	0.02	0.01	0.17	0.50	0.01	14.08	9.76	0.02
	Patigi	PTG-1E	79.57	9.87	1.90	0.01	0.27	0.16	0.14	2.91	0.37	0.01	26.68	8.06	0.29
	Rabba	RAB-1E	87.13	5.02	4.12	0.01	0.01	0.02	0.05	0.82	0.15	0.01	33.47	17.36	0.16
	Rabba	RAB-1F	90.84	4.62	3.16	0.01	0.04	0.06	0.08	0.53	0.12	0.02	38.50	19.66	0.11
	Rabba	RAB-1H	88.92	7.01	1.84	0.01	0.08	0.26	0.10	0.66	0.30	0.11	23.37	12.68	0.09
	Rabba	RAB-1L	78.58	12.17	1.98	0.01	0.18	0.25	0.16	0.94	0.72	0.02	16.90	6.46	0.08
	Rabba	RAB-1P	84.62	9.65	2.56	0.01	0.19	0.16	0.07	0.53	0.27	0.08	35.74	8.77	0.05
Published Standard	**PAAS**		62.80	18.90	4.52	0.11	2.20	1.30	1.20	3.70	1.00	0.16	18.90	3.32	0.20
	UCC		66.60	14.40	4.04	0.10	2.48	3.59	3.27	2.80	0.64	0.15	22.50	4.63	0.19

Table 4b: Trace Element Composition (ppm) of sandstone in the Northern Bida Basin with the Published Data (PAAS and UCC).

Sample No	La	Th	Co	Sc	Cr	Zr	Nb	Hf	Y	La/Th	La/Co	Th/Co	La/Sc	Cr/Th	Zr/Nb	Zr/Th	Zr/Sc	Zr/Hf	La/Y	Sc/Cr
AGB-1B	24.91	7.33	3.67	3.91	382.13	137.00	8.33	4.36	9.45	3.40	6.79	2.00	6.37	52.13	16.45	18.69	35.04	31.42	2.64	0.01
AGB-1D	56.16	17.86	4.37	9.92	341.34	499.64	26.89	14.77	26.95	3.14	12.85	4.09	5.66	19.11	18.58	27.98	50.37	33.83	2.08	0.03
AGB-1G	41.38	14.52	3.91	8.45	238.22	784.11	27.36	24.1	32.72	2.85	10.58	3.71	4.90	16.41	28.66	54.00	92.79	32.54	1.26	0.04
AGB-1K	49.21	12.84	4.04	6.46	314.03	596.80	22.82	17.89	28.37	3.83	12.18	3.18	7.62	24.46	26.15	46.48	92.38	33.36	1.73	0.02
ENG-1B	36.29	14.32	4.60	4.21	321.70	421.01	14.39	12.33	14.95	2.53	7.89	3.11	8.62	22.47	29.26	29.40	100.00	34.15	2.43	0.01
ENG-1E	30.80	10.28	3.13	2.69	238.4	181.18	7.09	4.66	5.4.38	3.00	9.84	3.28	11.45	23.19	25.55	17.62	67.35	38.88	0.00	0.01
ENG-1J	22.27	4.93	3.05	2.55	317.19	154.39	4.53	4.48	9.89	4.52	7.30	1.62	8.73	64.34	34.08	31.32	60.55	34.46	2.25	0.01
ENG-1L	18.22	9.61	3.05	4.75	198.60	271.19	9.50	8.19	10.44	1.90	5.97	3.15	3.84	20.67	28.55	28.22	57.09	33.11	1.75	0.02
ENG-1N	39.94	14.77	4.59	4.44	236.16	471.07	11.97	14.28	16.41	2.70	8.70	3.22	9.00	15.99	39.35	31.89	106.10	32.99	2.43	0.02
ENG-1V	49.19	20.59	2.78	4.49	331.16	902.83	18.06	26.61	30.99	2.39	17.69	7.41	10.96	16.08	49.99	43.85	201.08	33.93	1.59	0.01
KUD-1A	19.30	10.10	1.00	3.50	22.60	14.40	0.09	0.36	4.67	1.91	19.30	10.10	5.51	2.24	160.00	1.43	4.11	40.00	4.13	0.15
KUD-1B	21.00	12.30	1.70	4.90	78.40	18.90	0.12	0.42	4.99	1.71	12.35	7.24	4.29	6.37	157.50	1.54	3.86	45.00	4.21	0.06
KUD-1C	12.00	6.20	0.70	1.40	8.60	9.80	0.02	0.24	3.10	1.94	17.14	8.86	8.57	1.39	490.00	1.58	7.00	40.83	3.87	0.16
KUD-1F	12.80	11.00	0.70	2.40	22.30	18.40	0.09	0.48	4.26	1.16	18.29	15.71	5.33	2.03	204.44	1.67	7.67	38.33	3.00	0.11
KUT-2A	18.70	7.50	2.00	2.00	13.20	4.50	0.15	0.13	4.38	2.49	9.35	3.75	9.35	1.76	30.00	0.60	2.25	34.62	4.27	0.15
KUT-2D	4.70	3.60	1.50	1.40	8.00	3.50	0.08	0.09	0.95	1.31	3.13	2.40	3.36	2.22	43.75	0.97	2.50	38.89	4.95	0.18
KUT-2G	7.90	6.20	1.80	2.40	14.40	4.90	0.10	0.16	2.16	1.27	4.39	3.44	3.29	2.32	49.00	0.79	2.04	30.63	3.66	0.17
KUT-2K	14.60	8.00	1.20	2.30	14.20	4.20	0.05	0.16	4.17	1.83	12.17	6.67	6.35	1.78	84.00	0.53	1.83	26.25	3.50	0.16
SHG-1B	14.03	3.37	3.39	2.70	370.65	94.27	4.54	3.10	3.99	4.16	4.14	0.99	5.20	109.99	20.76	27.97	34.91	30.41	3.52	0.01
SHG-1K	17.97	4.39	3.03	2.54	397.77	139.59	4.62	4.73	7.10	4.09	5.93	1.45	7.07	90.61	30.21	31.80	54.96	29.51	2.53	0.01
SHG-1P	13.77	6.75	2.91	3.41	329.03	339.87	11.87	10.38	7.17	2.04	4.73	2.32	4.04	48.75	28.63	50.35	99.67	32.74	1.92	0.01
TAN-1A	10.52	2.88	3.47	3.10	247.03	101.94	2.84	3.52	4.70	3.65	3.03	0.83	3.39	85.77	35.89	35.40	32.88	28.96	2.24	0.01
TAN-1C	22.68	12.37	3.93	4.44	218.93	327.14	9.01	9.80	8.77	1.83	5.77	3.15	5.11	17.70	36.31	26.45	73.68	33.38	2.59	0.02
BDA-1A	18.79	4.88	3.37	3.30	258.88	166.29	6.37	4.26	4.74	3.85	5.58	1.45	5.69	53.05	26.11	34.08	50.39	39.04	3.96	0.01
BDA-1B	24.43	8.73	3.54	3.20	349.14	228.83	7.96	7.17	6.44	2.80	6.90	2.47	7.63	39.99	28.75	26.21	71.51	31.91	3.79	0.01
BDA-1D	14.65	8.25	4.31	3.05	390.01	304.71	4.53	9.03	4.59	1.78	3.40	1.91	4.80	47.27	67.26	36.93	99.90	33.74	3.19	0.01
BDA-1K	94.62	72.75	4.78	14.79	334.42	2527.15	86.87	74.60	44.60	1.30	19.79	15.22	6.40	4.60	29.09	34.74	170.87	33.88	2.12	0.04
BDA-1R	12.71	10.46	3.78	4.29	248.92	231.37	9.56	4.50	4.49	1.22	3.36	2.77	2.96	23.80	24.20	22.12	53.93	51.42	2.83	0.02
DOK-1D	24.10	18.99	3.52	4.49	189.74	874.86	16.61	24.61	17.89	1.27	6.85	5.39	5.37	9.99	52.67	46.07	194.85	35.55	1.35	0.02
DOK-1F	21.73	6.28	3.52	3.26	341.42	130.6	4.93	4.03	4.46	3.46	6.17	1.78	6.67	54.37	26.49	20.80	40.06	32.41	4.87	0.01
DOK-1K	16.91	4.29	3.92	2.76	269.05	114.95	4.20	3.68	3.12	3.94	4.31	1.09	6.13	62.72	27.37	26.79	41.65	31.24	5.42	0.01
DOK-1T	21.35	6.76	3.24	2.74	224.45	150.79	6.30	4.87	2.60	3.16	6.59	2.09	7.79	33.20	23.93	22.31	55.03	30.96	8.21	0.01
DOK-1X	27.56	7.60	2.80	2.94	223.67	247.84	6.51	7.72	4.71	3.63	9.84	2.71	9.37	29.43	38.07	32.61	84.30	32.10	5.85	0.01
GBL-1A	14.40	4.60	2.40	2.30	12.20	1.70	0.03	0.04	6.44	3.13	6.00	1.92	6.26	2.65	56.67	0.37	0.74	42.50	2.24	0.19
GBL-1C	13.00	4.20	1.20	1.60	9.80	1.20	0.02	0.04	4.54	3.10	10.83	3.50	8.13	2.33	60.00	0.29	0.75	30.00	2.86	0.16
GBL-1D	16.50	14.20	1.70	2.90	13.30	3.80	0.03	0.12	4.61	1.16	9.71	8.35	5.69	0.94	126.67	0.27	1.31	31.67	3.58	0.22
GBL-1E	24.90	4.00	4.50	1.50	4.90	0.40	0.02	0.02	14.46	6.23	5.53	0.89	16.60	1.23	20.00	0.10	0.27	20.00	1.72	0.31
GBU-1A	7.80	7.00	1.20	3.30	12.50	3.60	0.02	0.12	2.50	1.11	6.50	5.83	2.36	1.79	180.00	0.51	1.09	30.00	3.12	0.26
GBU-1B	56.00	7.90	1.40	2.50	8.70	2.80	0.02	0.06	8.18	7.09	40.00	5.64	22.40	1.10	140.00	0.35	1.12	46.67	6.85	0.29
GBU-1D	26.10	4.60	0.90	1.30	8.40	1.70	0.03	0.04	3.13	5.67	29.00	5.11	20.08	1.83	56.67	0.37	1.31	42.50	8.34	0.15
PTG-1A	24.40	8.10	1.40	1.50	8.40	2.90	0.03	0.08	4.07	3.01	17.43	5.79	16.27	1.04	96.67	0.36	1.93	36.25	6.00	0.18
PTG-1B	17.70	14.20	1.10	1.60	14.80	4.90	0.03	0.13	4.54	1.25	16.09	12.91	11.06	1.04	163.33	0.35	3.06	37.69	3.90	0.11
PTG-1D	4.10	14.50	3.30	2.90	88.20	9.80	0.15	0.26	1.23	0.28	1.24	4.39	1.41	6.08	65.33	0.68	3.38	37.69	3.33	0.03
PTG-1E	14.10	4.40	1.60	1.90	9.60	1.10	0.02	0.03	6.81	3.20	8.81	2.75	7.42	2.18	55.00	0.25	0.58	36.67	2.07	0.20
RAB-1E	6.77	2.72	4.71	3.64	309.76	154.30	4.14	6.75	8.09	2.49	1.44	0.58	1.86	113.88	37.27	56.73	42.39	22.86	0.84	0.01
RAB-1F	9.77	3.06	3.07	3.34	314.4	60.21	2.98	2.08	4.02	3.19	3.18	1.00	2.93	102.75	20.20	19.68	18.03	28.95	2.43	0.01
RAB-1H	13.92	3.82	3.10	3.21	301.67	146.83	7.02	4.71	6.33	3.64	4.49	1.23	4.34	78.97	20.92	38.44	45.74	31.17	2.20	0.01
RAB-1L	30.81	11.14	3.16	4.24	229.15	453.15	16.41	14.28	9.81	2.77	9.75	3.53	7.27	20.57	27.61	40.68	106.88	31.73	3.14	0.02
RAB-1P	11.91	3.87	3.31	3.35	299.05	110.60	6.95	3.23	4.54	3.08	3.60	1.17	3.56	77.27	15.91	28.58	33.01	34.24	2.62	0.01
PAAS	38.20	14.60	23.00	16.00	110.00	210.00	19.00	4.00	27.00	2.62	1.66	0.63	2.39	7.53	11.05	14.38	13.13	52.50	1.41	0.15
UCC	31.00	10.50	17.30	14.00	92.00	193.00	12.00	4.30	21.00	2.95	1.79	0.61	2.21	8.76	16.08	18.38	13.79	44.88	1.48	0.15

Table 4c: Rare earth element (REE) concentrations of sandstone samples in the Northern Bida Basin with the published (PAAS and UCC) data.

Sample No.	La	Ce	Pr	Nd	Sm	Eu	Gd	Tb	Dy	Ho	Er	Tm	Yb	Lu	_	ΣLREE	ΣHREE	ΣLREE/ΣHREE	Eu/Eu*
AGB-1B	24.91	50.74	6.14	21.74	3.98	0.75	3.07	0.45	2.24	0.43	1.08	0.14	0.91	0.14	117.72	108.51	8.46	12.83	0.08
AGB-1D	56.16	104.39	12.94	46.49	8.32	1.53	6.62	1.02	4.39	1.11	2.98	0.42	2.88	0.45	251.70	229.30	20.87	10.99	0.04
AGB-1G	41.38	84.88	9.50	30.57	4.83	0.86	4.31	0.83	4.53	1.25	3.6	0.55	3.96	0.65	192.70	171.16	20.68	8.28	0.06
AGB-1K	49.21	96.13	10.95	39.92	7.68	1.47	6.54	1.04	5.72	1.17	3.06	0.43	2.83	0.42	226.57	203.89	21.21	9.61	0.04
ENG-1B	36.29	78.54	8.09	28.37	4.83	0.70	4.42	0.63	3.07	0.65	1.68	0.27	1.94	0.32	169.8	156.12	12.98	12.03	0.05
ENG-1E	30.80	69.05	6.42	21.63	3.40	0.55	3.22	0.42	2.02	0.41	0.99	0.16	1.11	0.17	140.35	131.30	8.50	14.45	0.07
ENG-1J	22.27	39.93	4.11	13.18	2.24	0.37	2.23	0.36	1.89	0.40	1.03	0.17	1.21	0.20	89.59	81.73	7.49	10.91	0.10
ENG-1L	18.22	32.02	3.40	11.58	1.95	0.35	1.94	0.34	1.97	0.44	1.20	0.20	1.52	0.26	74.39	67.17	7.87	8.53	0.13
ENG-1N	39.94	94.39	7.97	26.83	4.49	0.70	4.33	0.62	3.23	0.67	1.72	0.27	1.86	0.31	187.33	173.62	13.01	13.35	0.05
ENG-1V	49.19	87.32	10.24	34.43	4.97	0.79	4.85	0.97	4.39	1.20	3.29	0.53	3.82	0.60	209.59	187.15	21.65	8.64	0.03
KUD-1A	19.30	38.80	4.22	17.43	3.23	0.54	1.96	0.21	1.36	0.19	0.56	0.07	0.53	0.07	88.47	82.98	4.95	16.76	0.12
KUD-1B	21.00	43.10	4.50	17.19	2.94	0.57	1.87	0.21	1.44	0.24	0.66	0.07	0.64	0.08	94.51	88.73	4.21	17.03	0.14
KUD-1C	12.00	34.80	2.24	8.59	1.69	0.21	0.73	0.11	0.71	0.11	0.29	0.03	0.30	0.04	62.85	60.32	2.32	26.00	0.23
KUD-1F	12.80	54.00	2.70	11.00	2.06	0.30	1.02	0.13	0.73	0.13	0.40	0.05	0.35	0.05	84.72	82.56	2.86	28.87	0.20
KUT-2A	18.70	58.60	3.09	12.98	1.85	0.28	1.01	0.13	0.77	0.12	0.35	0.04	0.34	0.02	98.28	94.22	2.78	34.25	0.21
KUT-2D	4.70	19.10	0.73	3.06	0.50	0.05	0.27	0.04	0.17	0.02	0.06	0.02	0.07	0.02	28.81	28.09	0.67	41.93	0.51
KUT-2G	7.90	33.20	1.50	6.09	0.96	0.14	0.62	0.06	0.48	0.05	0.22	0.02	0.18	0.02	51.44	49.65	1.65	30.09	0.32
KUT-2K	14.60	28.20	3.02	11.89	2.31	0.30	1.28	0.14	0.94	0.13	0.32	0.04	0.37	0.04	63.58	60.02	3.26	18.41	0.14
SHG-1B	14.03	24.06	2.20	6.69	1.04	0.17	0.95	0.14	0.77	0.16	0.41	0.06	0.46	0.08	52.22	49.02	3.03	16.18	0.24
SHG-1K	17.97	37.37	2.97	9.24	1.63	0.2	1.61	0.27	1.36	0.28	0.7	0.11	0.79	0.12	74.62	69.18	5.24	13.20	0.10
SHG-1P	13.77	27.01	2.74	9.18	1.47	0.21	1.39	0.21	1.17	0.27	0.75	0.12	0.91	0.16	59.36	54.17	4.98	10.88	0.14
TAN-1A	10.52	96.09	2.38	8.38	1.53	0.32	1.36	0.22	1.08	0.22	0.53	0.08	0.57	0.09	123.37	118.90	4.15	28.65	0.21
TAN-1C	22.68	41.17	4.68	14.71	3.16	0.61	2.67	0.44	2.33	0.49	1.23	0.21	1.54	0.24	97.16	87.40	94.15	9.55	0.10
BDA-1A	18.79	51.76	3.21	9.79	1.41	0.27	1.12	0.18	0.94	0.21	0.57	0.09	0.59	0.10	89.03	84.96	3.80	22.36	0.24
BDA-1B	24.43	78.81	4.56	14.02	2.24	0.34	1.71	0.25	1.25	0.26	0.70	0.10	0.73	0.12	130.52	124.06	4.12	24.43	0.12
BDA-1D	14.65	42.68	2.82	8.84	1.37	0.17	1.08	0.15	0.84	0.18	0.52	0.08	0.58	0.10	74.06	71.36	3.53	20.22	0.16
BDA-1K	94.62	190.32	20.73	70.08	11.97	0.78	9.20	1.40	7.48	1.66	4.89	0.77	4.80	0.99	420.69	387.72	32.19	12.04	0.01
BDA-1R	12.71	24.34	2.20	6.87	1.08	0.13	0.89	0.15	0.88	0.20	0.61	0.10	0.72	0.12	52.00	48.20	3.67	13.13	0.19
DOK-1D	24.10	36.99	4.06	12.78	2.03	0.33	1.87	0.37	2.55	0.61	1.83	0.29	2.16	0.39	90.36	79.96	10.07	7.94	0.05
DOK-1F	21.73	43.77	4.40	14.22	2.12	0.41	1.44	0.21	0.92	0.18	0.45	0.06	0.41	0.07	90.39	86.24	3.74	23.06	0.13
DOK-1K	16.91	31.10	3.10	10.11	1.55	0.34	0.98	0.14	0.67	0.14	0.37	0.05	0.37	0.06	64.89	62.77	2.78	22.58	0.04
DOK-1T	21.35	27.96	2.98	8.14	1.13	0.21	0.79	0.11	0.54	0.11	0.32	0.05	0.34	0.05	64.08	61.56	2.31	26.65	0.30
DOK-1X	27.56	54.97	4.81	18.81	2.82	0.49	1.90	0.26	1.23	0.25	0.67	0.10	0.69	0.12	116.68	110.97	4.22	21.26	0.15
GBL-1A	14.40	24.30	2.65	9.76	1.30	0.28	1.37	0.18	0.82	0.19	0.54	0.08	0.47	0.07	57.41	53.41	3.72	14.36	0.22
GBL-1C	13.00	28.70	2.86	10.09	1.52	0.33	1.31	0.18	0.94	0.20	0.50	0.07	0.35	0.06	60.11	56.17	3.61	14.56	0.23
GBL-1D	16.50	51.10	3.69	12.77	2.16	0.33	1.74	0.23	1.15	0.21	0.57	0.08	0.48	0.07	91.08	86.22	4.53	19.03	0.12
GBL-1E	24.90	36.80	4.82	20.65	3.56	0.88	2.77	0.44	2.59	0.49	1.28	0.22	1.01	0.13	101.54	91.73	8.93	10.27	0.12
GBU-1A	7.80	14.40	1.51	4.61	0.70	0.16	0.63	0.10	0.51	0.09	0.25	0.04	0.24	0.03	31.07	29.02	1.89	14.35	0.50
GBU-1B	56.00	114.00	13.93	46.35	7.75	1.57	4.64	0.60	2.51	0.38	0.83	0.12	0.74	0.08	249.50	238.03	9.90	24.04	0.06
GBU-1D	26.10	129.20	6.51	21.58	3.77	0.85	2.10	0.28	1.09	0.14	0.33	0.05	0.23	0.02	192.25	187.16	4.24	44.14	0.15
PTG-1A	24.40	52.10	4.61	19.02	2.87	0.63	2.24	0.27	1.23	0.22	0.55	0.05	0.45	0.05	110.69	104.00	4.06	20.75	0.13
PTG-1B	17.70	36.80	3.31	10.85	1.82	0.20	1.42	0.18	0.85	0.18	0.39	0.06	0.36	0.06	74.18	70.48	3.50	20.14	0.11
PTG-1D	4.10	11.30	0.96	3.28	0.60	0.10	0.36	0.07	0.26	0.06	0.14	0.03	0.18	0.02	21.46	20.24	1.12	18.07	0.64
PTG-1E	14.10	23.60	3.45	11.50	1.95	0.39	1.53	0.25	1.29	0.24	0.69	0.11	0.62	0.08	59.80	54.60	4.81	11.35	0.18
RAB-1E	6.77	17.69	1.97	7.69	1.69	0.41	1.61	0.30	1.60	0.34	0.88	0.14	1.07	0.16	42.32	34.81	6.10	4.87	0.21
RAB-1F	9.77	13.24	2.18	7.77	1.56	0.39	1.41	0.23	1.22	0.25	0.64	0.10	0.70	0.10	39.56	34.52	4.65	7.42	0.24
RAB-1H	13.92	36.64	2.52	8.42	1.52	0.36	1.46	0.25	1.27	0.27	0.69	0.11	0.82	0.13	68.38	63.02	4.00	12.6	0.22
RAB-1L	30.81	54.30	6.96	24.14	4.17	0.43	3.58	0.45	1.97	0.41	1.04	0.17	1.26	0.21	130.9	121.38	9.09	13.35	0.04
RAB-1P	11.91	18.89	2.20	4.59	1.35	0.28	1.23	0.20	1.06	0.23	0.62	0.10	0.67	0.10	46.13	41.64	4.21	9.89	0.23
PAAS	38.20	79.60	8.83	33.90	4.55	1.08	4.66	0.77	4.68	0.99	2.85	0.41	2.82	0.43	184.77	166.08	17.61	9.43	0.71
UCC	31.00	63.00	7.10	27.00	4.70	1.00	4.00	0.70	3.90	0.83	2.30	0.30	2.00	0.31	148.14	132.80	14.34	9.26	0.66

***Average Post Archean Au stralian Shale (PAAS) values after McLennan (2001)**

****Average upper continental crust values (UCC) after McLennan (1989)**

supported the rift model idea. However, Braide (1992) suggested a wrench fault tectonic model for the origin of the basin.

The stratigraphy of the Bida Basin has been documented by Adeleye and Dessauvagie (1972) in the central parts of the basin around Bida. Four mappable stratigraphic unites are recognized in this area namely, the Bida Sandstone (divided into the Doko Member and the Jika Member), the Sakpe Ironstone, the Enagi Siltstone, and the Batati Formation. These are correlatable with the stratigraphic units in the Southern Bida Basin. In the southern Bida Basin, exposures of sandstones and conglomerates of the Lokoja Formation directly overly the basement rock comprises of gneisses and schist. This is overlain by the alternating shales, siltstones, claystones and sandstones of the Patti Formation and capped by ironstones of the Agbaja Formation.

The southern Bida Basin has witnessed more research contributions to better understand especially in the area of geology, depositional history and paleogeography. Adeleye (1973) documented the geology while Jan du Chene et al. (1979) on the micropaleontological studies of Patti Formation reported palynomorph and foraminiferal assemblages. Ojo and Akande (2003) documented an occasional marine influence during the deposition of Campanian Lokoja Formation sediments, thus, interpreted the paleoenvironments as alluvial fan to shallow marine type. Akande *et al.,* (2005) interpreted the paleoenvironments of the sedimentary successions in the southern Bida Basin as ranging from continental to marginal marine and marsh environments for the Cretaceous lithofacies. Ojo and Akande (2009) concluded that Lokoja Formation was deposited in an environment dominated by continental processes ranging from well developed proximal alluvial fan, braided channel and pockets of floodplains. Ojo (2010) studied the palynomorphs assemblages and paleoenvironments of the Patti Formation and dated the shaly facies as Maastrichtian age.

Meanwhile, lesser research work has been documented in the northern part of the basin. The following researchers have contributed especially in the area of sedimetology and paleogegraphy; Olaniyan and Olobaniyi (1996) studied the sedimentology and stratigraphy of Kajita, north of River Niger and suggested fluvial environments for the sandstones and the conglomerates. More recently, Ojo (2012) suggested fluvial processes of deposition for the Bida Formation sediments around Share-Patigi area. He also suggested an uplifted continental block provenance and short transportational history for the prevalent facies in the area. By this it shows that, the geology of the northern Bida Basin has not been well described and documented as compared with the southern Bida Basin. Therefore, the present study aims at evaluating the quantitative facies and geochemical analysis in order to establish the lithofacies units for regional correlation and describe provenance for better sedimentary-tectonic framework understanding on the basin origin.

MATERIALS AND METHODS

The fieldwork was conducted on the exposed outcrop sections within northern Bida Basin by careful bed by bed study and sedimentological information was transformed into detail graphical logs. Facies analysis of the studied lithological sections was attempted following Miall (1977; 1985; 1996) scheme to determine facies association and architecture elements for depositional environment interpretations. Fresh, representative samples were collected at different depth and horizon from 17 lithological sections (Figure 2) were properly stored in the sample bag and labeled for laboratory analysis including geochemical and zircon image analysis at the National Geophysical Research Institute (NGRI), Hyderabad, India.

The determination of major elemental composition on 50 selected samples was carried out by the standard laboratory analytical procedure of x-ray fluorescence (XRF) and inductively coupled plasma-mass spectrometry (ICP-MS). During analysis, the accuracy and precision of the method was monitored with control samples and duplicates by running USGS international standard reference materials (SRMs) viz., GSR-4, GSR-6, GXR-6 to correct long-term instrument drift. The error of replicate analyses was 1-2% better than all analyzed trace and rare earth elements. Six sandstone samples were also selected for zircon morph-typological analysis; three (3) samples each from two locations; Agbonna ridge, Share and Doko ridge, Doko. Prior to the image acquiring, about 3-4 kg of freshly collected sediment samples were sieved for the fraction proportion smaller than 2 mm, then zircon grains were concentrated by a combination of Wilfley shaker table and then handpicked under binocular microscope (ZEISS Stemi 2000-C). The zircon grains were mounted in vacuum-grade epoxy resin discs, diamond-polished down to about half of their thickness for analysis. However, the zircon crystal morphology was studied after zircon grains were polished to expose their centers and imaged. In order to get pictures of zircon grains with a very high resolution and magnification, a scanning electron microscope was used in the back scattered electron (BSE) mode. Cathodoluminescence (CL) images were obtained using VEGA3 TESCAN SEM-CL. The zircons were imaged at a working distance of 14-17 mm and accelerating voltage of 20-21 kV. For each of the samples studied, the typologic distribution was based on examination of at least 300 unbroken zircon crystals from each sample.



Figure 3a: Field photograph showing typical clast-supported, massive conglomerate (Gcm) and matrix-supported, massive conglomerate (Gmm) sub-facies at: (i) Proposed Harmattan Patigi University site, Patigi (Longitude: 08°42'53.5"N; Latitude: 005°46'55.7"E); and (ii) Baganko village, near Abiola farm, Lafiagi area (Longitude: 08°54'29.4"N; Latitude: 005°19'24.6"E).

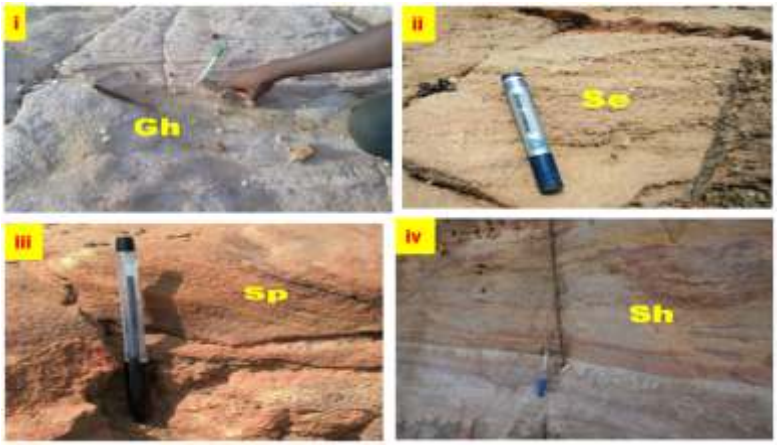


Figure 3b: Field photograph showing typical; (i) crudely bedded conglomerate (Gh) sub-facies at the middle part of section at Shonga, along Tada road (Longitude: 005°08'50.1"E; Latitude: 09°01'27.4"N); (ii) crudely stratified sandstone (Se) sub-facies at the lower part of section at Wushishi, near River Kaduna (Longitude: 006°24.956'E; Latitude: 08°37.371'N); (iii) planar cross-stratified sandstone (Sp) sub-facies at the middle part of Agbonna ridge, Share (Longitude: 004°58'36.3"E (Latitude: 08°49'32.3"N); (iv) horizontally stratified sandstone (Sh) sub-facies at the upper part of the exposure near railway at Baro (Longitude: 006°24.956'E; Latitude: 08°37.371'N).

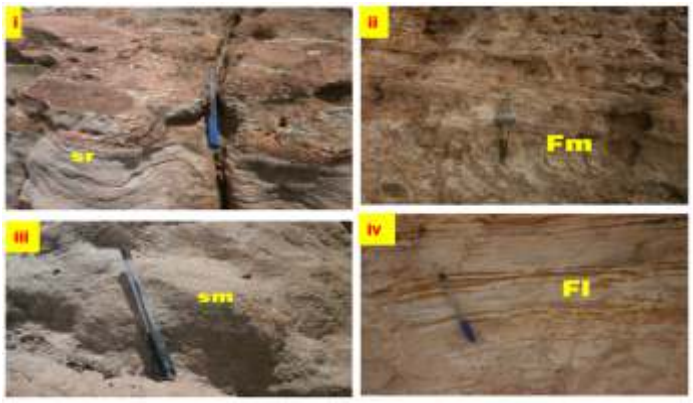


Figure 3c: Field photograph showing typical example of; (i) a rippled cross-stratified sandstone (Sr) sub-facies at Dokko ridge, near Police Station (Longitude: 005°37.545'E; Latitude: 08°56.744'N); (ii) a massive mudstone (Fm) sub-facies at Kutigi (Longitude: 005°35.43' E; Latitude: 09°12.03' N); (iii) massive sandstone (Sm) sub-facies at Tanagi ridge, along Mokwa-Kaduna road (Longitude: 005°43.798' E; Latitude: 09°55.342' N) and (iv) finely laminated mudstone (Fl) sub-facies at Tanagi (Longitude: 005°43.798' E; Latitude: 09°55.342' N).

RESULT PRESENTATIONS

Facies Analysis

Litho and Sub-facies

The facies description of Seventeen (17) outcrop lithological sections is based on the observed physical processes of the sediments during and after deposition. Ten sub-facies; clast-supported, massive conglomerate (Gcm), matrix-supported, massive conglomerate (Gmm), clast-supported, crudely bedded conglomerate (Gh), crudely stratified (Se), planar cross-stratified sandstone (Sp), rippled stratified sandstone (Sr), horizontally stratified sandstone (Sh), massive sandstone (Sm), finely laminated mudstone (Fl) and massive mudstone (Fm) arranged into distinctive cycles and associations were identified within the study area (Table 2) using the Miall (1985, 1996) classification schemes.

Clast-supported, massive conglomerate (Gcm) sub-facies

The clast-supported, massive conglomerate (Gcm) sub-facies is composed of sub-rounded to rounded pebble size clasts and granules (0.3 to 14.0cm in diameter), mainly quartz, commonly occurs within beds of 0.5 to 3.0 meters thick. This sub-facies is closely compared with Orthoconglomerate of Pettijohn (1957). The bed's thickness implies the operation of mass-flows of considerable magnitude with rolling bedload of the large clasts along a bed and it's suggested to be a deposit from traction by a unidirectional current. Majority of the clasts with ordered imbricated fabric lie tangential to bedding (Figure 3ai). The shape and size of the sandwiched clasts also reflect a high discharge and higher energy of the depositional current. An occasional gradation from Gcm to Gmm and Gh (coarse sub-facies) was observed (Figure 3aii) which indicate diminish of flow energy strength and in support of deposition from a single current according to Walker (1978). It is usually observed in lower and upper parts of the lithological sections exposed at the proposed Harman-Patigi University, Patigi and behind Baganko village, near Abiola farm (Lafiagi area).

Matrix-supported, massive conglomerate (Gmm) sub-facies

The matrix-supported, massive conglomerate (Gmm) sub-facies are generally supported by poorly sorted, coarse-grained sandstone matrix for the clasts (Figure 3aii). It is otherwise referred to as Paraconglomerate by Pettijohn (1957). Individual beds of Gmm ranges between 0.2 and 1.0m thick with sharp bases and the clasts present are usually of size range between 1.7 and 8.7cm in diameter. The clasts sitting in a poorly sorted matrix are mostly sub-angular to rounded, non-imbricated granules to pebbles (mainly quartz and schist) which usually decrease upward in each cycle (Figure 3aii). Its generation may be connected with the result of catastrophic flooding events, during which channels formed and they were filled with poorly sorted or unsorted coarse materials as it display relatively high-hydraulic properties which is attributed to a gravel-dominated braided rivers in a fluvial system according to Smith (1974) and Miall (1977). Typical Gmm sub-facies were observed at the following exposed lithological sections; middle part of the outcrop sections at proposed Harman-Patigi University, Patigi, Baganko village, near Abiola farm (Lafiagi area), at Lade along Gbugbu-Patigi road, Share town, Shonga town, Patti-Chin and Baro.

Crudely bedded conglomerate (Gh) sub-facies

The crudely bedded conglomerate (Gh) is composed of few sub-angular to sub-rounded, poorly sorted gravel lenses that floats within the sand matrix with grading exhibiting an abrupt upward transition into Gcm and Gmm sub-facies. The beds thickness ranges from 0.3 to 0.8m. In few occasions, Gh sub-facies consists of stratified gravels that commonly infill channelized erosive basal surfaces and the gradational top contact (Figure 3bi). Due to the crudely bedded nature of Gh sub-facies beds, it is interpreted to represent the accretion of gravel in longitudinal bars which usually begins with the largest clasts as diffuse gravel sheets according to Cant (1982). This attributes like Gcm and Gmm sub-facies indicate gravel-dominated braided rivers in a fluvial system according to Smith (1974). Gh sub-facies were observed in the middle and lower parts of the exposed outcrops at Shonga, Zambufu, Gbedeworo, Gbugbu, Wariku, Lafiagi, Baganko and Baro, all in the south-eastern part of the northern Bida Basin.

Crudely stratified sandstone (Se) sub-facies

The crudely stratified to massive sandstone (Se) sub-facies is composed of sands and minor silts, medium sorted and occur only at the lower and middle parts of the studied sections (Figure 3bii). It consists of sub-angular to sub-rounded extraformational and isolated pebble clasts within the bodies of sandstones grains. The thickness of each bed varies between 0.5m to 2.0m and commonly passes upward into coarser bed with lower boundary usually gradational with facies Gh. The bottom contacts are erosional, causing undulatory, concave up bases while the tops of the beds are commonly gradational into facies Sp and Sh. Association of Se and Sm sub-facies in some locations (e.g. Rabba, Bida, Wushishi, Baro, Lemu, Dokko) is suggestive of development of low sinuosity channel bars arising from channel switching, and lack of point bar sedimentation here suggests an upper flow regime during transportation according to Miall (1988). This sub-facies could be deposited by a moderately to high-energy environment from channels of the main fluvial channel system. Se sub-facies were observed in the exposed outcrops within the central part of the study area including Share, Shonga, Rabba, Bida, Enagi, Wushishi, Baro, Lemu and Dokko.

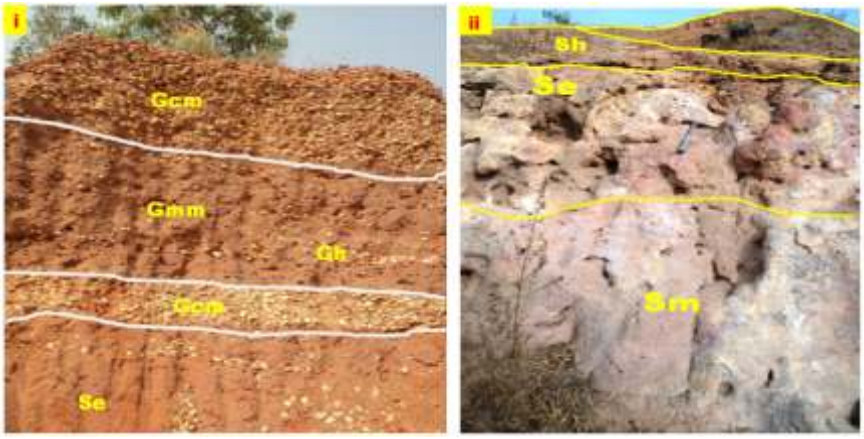


Figure 4a: Field photograph showing typical example of; (i) outcrop facies association 1 (OFA1) that are preserved fluvial Channel lags (Longitude: 08°42'53.5"N, Latitude: 005°46'55.7"E; Longitude: 08°54'29.4"N, Latitude: 005°19'24.6"E), (ii) outcrop facies association 2 (OFA2) that are preserved as braided fluvial channel at Shonga, Lafiagi, Lade, Patti-Wodata, Kajita, Rabba, Bida, Dokko, Jimma, Patti-Chin, Wushishi and Lemu (Longitude: 005°08'50.1"E, Latitude: 09°01'27.4"N; Longitude: 005°56.090'E, Latitude: 08°58.994'N; Longitude: 005°37.545'E, Latitude: 08°56.744'N; Longitude: 08°42'45.2"N; Latitude:006°02'51.9"E)

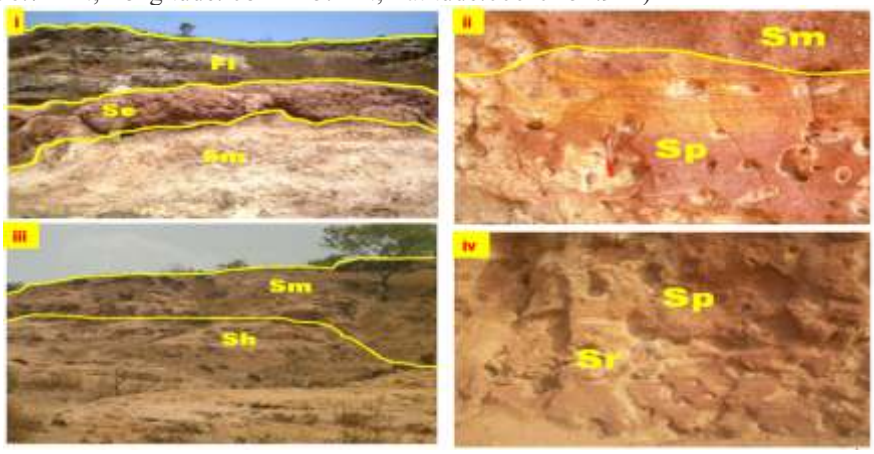


Figure 4b: Field photograph showing typical example of; (i) outcrop facies association 3 (OFA3) that are well preserved as a meandering channels sandstones and are well preserved at Shonga, Lafiagi and Bida (Longitude: 09°04.449'N, Latitude: 006°14.018'E; Longitude: 08°50'44.0"N, Latitude: 005°25'03.0"E; Longitude: 005°59.98' E, Latitude: 09°05.98' N) and (ii) outcrop facies association 4 (OFA4) that are well preserved as tidally influenced fluvial channel sandstone and are well preserved at Manigi, Rabba, Enagi and Wushishi (Longitude: 005°32.277' E; Latitude: 09°46.599' N; Longitude: 005°35.43' E, Latitude: 09°12.03' N; Longitude: 006°03.846'E, Latitude: 09°43.621'N)



Figure 5a: An outcrop showing a typical characteristic of; (i) a Gravel Bars and Bedform & Sandy Bedform Elements at Baganko (Longitude: 08°54'29.4"N, Latitude: 005°19'24.6"E) and (ii) at Ndeji (Longitude: 08°54'29.4"N, Latitude: 005°19'24.6"E).

Planar cross-stratified sandstone (Sp) sub-facies

The planar cross-stratified sandstone (Sp) sub-facies comprises of very coarse- to fine-grained sandstone which are arranged into lenticular or tabular sets up to 12.0m thick and characterized internally by planar cross-stratification (Figure 3biii). The beds which are usually tabular commonly occur laterally and each bed having thickness ranging from 2.0 to 15.0m. The upper and lower boundaries of Sp sub-facies are gradational and the bounding surfaces may be traced for tens of meters. The beds in few occasions appeared well lithified (e.g. Enagi, Jima, Doko and Kajita). Sp sub-facies are interpreted as the product of straight crested 2D dunes which are common in shallow sandbed braided rivers. The down-current dipping cross-strata are common with the cosets containing regularly spaced sets of cross-stratification 2-5 cm thick on low angle bounding surfaces. The foresets dip often diverges strongly from the dip of bounding surfaces by 30°-60°. The occurrence of this facies commonly in the southeastern, southwestern and central parts is suggested to have formed by deposition from traction in a low-energy, unidirectional current or the deposition in small channel infills as reported by Miall (1996). Sp sub-facies were observed in Agbonna ridge at Share, road-side exposures at Gbedeworo and Lafiagi and a ridge at Lemu. The sub-facies is also present at the ridge in Kutigi, Jimma, Dokko, Kajita, Bida, Tanagi and at the river cut exposure in Rabba, near Mokwa.

Horizontally stratified sandstone (Sh) sub-facies

The horizontally stratified sandstone (Sh) sub-facies is composed of coarse-, medium- and fine-grained sandstone, with fine laminae arranged into thin beds possessing a parting lineation defined mica (muscovite) intercalations (Figure 3biv). Individual beds range from 0.2 to 8.0m in thickness with gradational tops and bases. The Sh sub-facies have been observed grading upwards into Sr sub-facies. The grain size profiles generally fine-upward, are rarely irregular due to apparently random interlamination and stacking of alternating lithologies, thus, record a rapid change in flood regime that recognizes a high energy situation followed by waning of the flow and fallout of finer particles. The horizontal cosets of approximately 2.0m thick within the Sh sub-facies with lenticular or irregularly wedge-shaped beds is well compared with the large 3D dunes (mega-ripples) and small dunes of shallow sandbed braided rivers suggested by Collinson (1970), Smith (1970, 1971, 1972). Sh sub-facies could be deposited via high-energy that spilled into a lower energy environment from channels during flooding of the main fluvial channel system according to Miall (1996), Prothero and Schwab (2004). This sub-facies was observed at the lithological sections at Share (Agbonna ridge), Rabba, Bida, Enagi, Kutigi, Tanagi, Lemu, Doko and Wodata.

Rippled cross-stratified sandstone (Sr) sub-facies

The rippled stratified sandstone (Sr) sub-facies comprise few centimeters to meters thick rippled cosets and bedsets of sandstone and commonly observed at the middle and upper parts of the studied outcrops (Figure 3ci). The thickness of single beds of this sub-facies varies between 0.2m to 2.50m and may or may not show an erosive lower surface, but the upper contact is often irregular. The ripples represent lower flow regime unidirectional traction currents which can also be formed as a result of rapid deposition of grains from suspension in fluvial environments. The Sr sub-facies may also be deposited from presence of a subtle primary-current lineation and under lower flow velocities according to Prothero and Schwab (2004). The lithological sections that show typical characteristics of the Sr sub-facies were observed in the lower part of Agbonna ridge at Share, the middle part of Shonga ridge and exposure in Rabba near Mokwa.

Massive sandstone (Sm) sub-facies

The massive sandstone (Sm) sub-facies comprise beds of non-organize sandstone, usually of centimeters to meters thick (Figure 3ciii). The thickness of single beds varies between 2.0 and 5.0m and may contain sub-rounded to rounded, floating pebbles. This grain size result is a characteristic of low to medium energy of deposition in a fluvial environment. The Sm sub-facies is suggested to have formed by very rapid sedimentation, probably by high discharge events such as sheet-floods or as as a result of rapid deposition of grains from saltation in fluvial environments as suggested by Miall (1996). Sm sub-facies are well exposed in the most of the outcrops found in the south-eastern, south-western and central parts of the study area. For example, they were observed at the upper part of the Agbonna ridge, at the middle and upper parts of Shonga, Jima, Doko, Kajita, Enagi and Lemu ridges. The sub-facies were also observed at the middle and upper parts of the road cut exposures in Lafiagi and at the middle and upper parts of the river side exposure at Rabba near Mokwa.

Massive very fine sandstone and mudstone (Fm) sub-facies

The massive mudstone (Fm) sub-facies mainly composed of massive siltstone, claystone and minor very fine grained sandstone. It is composed of varying colorations; whitish to brownish (Figure 3cii). The lower boundary is commonly irregular due to the underlying topography while the upper boundary usually flat and always lacks any observable sedimentary structure. Each bed unit ranges in thickness from 0.2m to 10.0m with the profiles ranges from 10 to 50.0m and like Fl sub-facies. Fm sub-facies is generally massive and homogeneous which suggested to be formed because of rapid deposition from suspension in overbank settings or to lack of platy grains. Like Fl sub-facies, Fm also shows evidence of deposition from suspension settling of fine-grained sandstone, silt-

and clay- sized particles, which may have been formed in overbank and floodplain environments. The alternating siltstone and claystone, indicates widespread deposition from suspension over the upper parts of sandy bedforms or across low relief, abandoned flood plains. Fl sub-facies usually exposed in association with Fm sub-facies and commonly found in the most of the outcrops in the northern and central parts of the northern Bida Basin. They were studied at the middle and upper parts of the ridges in Share, Gbugbu, Kutigi, Enagi, Rabba and Manigi.

Finely laminated mudstone (Fl) sub-facies

The finely laminated mudstone (Fl) sub-facies are composed mostly of laminated siltstone and claystone beds with erosional or sharp laminae boundaries (Figure 3civ). The lower and upper boundaries are generally sharp and planar with each bed unit ranges in thickness from 2.0 to 4.0 m. The sub-facies are composed mostly of whitish to light brown, occasionally interlaminated siltstone, clayey-siltstone and very fine-grained sandstone with thickness of each units varies from 0.5 to more than 1.0 meter. Typically this sub-facies is sharply topped by Sm or Sh, sub-facies. Fl sub-facies contains little evidence of bedload deposition and is interpreted as deposition from suspension settling of fine to very fine-grained sandstone, silt- and clay-sized particles, which may have been flocculated and formed in overbank and floodplain environments. The alternating siltstone-claystone in some parts of the area may indicate widespread deposition from suspension across low relief, abandoned flood plains. Finely laminated mudstone sub-facies are well exposed in the exposed outcrops within northern and central (as intebeddings) parts of the study area. The location where the typical characteristics were observed includes; the middle and upper parts of the Agbonna ridge at Share and other ridges at Kutigi, Enagi, Rabba, Tanagi and Manigi.

Outcrop Facies Association Analysis and Characteristics

Facies associations are assemblages of spatially and genetically related facies, distinguished as the principal "building blocks" of the sedimentary succession (Collinson, 1996). According to Miall (1977) and Collinson (1999), the grouping and interrelationship characteristic of adjacent facies is very important in depositional environment and succession interpretations because of ambiguity nature of facies. The five interpreted outcrop facies associations (OFA) described in this study was based on the combinations of facies using their genetic variations and interrelationship.

Outcrop Facies Association 1 (OFA1)

The outcrop facies association 1 (OFA1) comprises of major conglomerates sub-facies (Gcm, Gmm and Gh). Occasionally, subordinate sandstone (Se) sub-facies occur laterally as confined, lenticular bodies in an assocciation with OFA1. The typical lithological sections with OFA1 composed angular clast sized constituents which suggest a channel lags deposits. The basal contact is usually erosional and commonly displays a poorly sorted, conglomeratic base. The basal surfaces of this facies association were observed to have eroded down many meters into the underlying sediment. The individual bodies can form larger deposits with highly variable morphology ranging from small (~5 meters thick, ~10 meters wide) to a large (10 meters thick, ~20 meters wide) channelized body. OFA1 is interpreted as fluvial deposit. The preserved conglomeratic bed suggests a migration of longitudinal and transverse bars during maximum discharge in the rivers according to Miall (1996). The OFA1 is predominant in the stratigraphic sections at the proposed Harman Patigi University, Patigi (Figure 4ai) and at the exposed section at Baganko village (Figure 3ai). Also, minor OFA1 were aboserved at Gbugbu and Gbale all along Share-Gbugbu road.

Outcrop Facies Association (OFA2)

The outcrop facies association 2 (OFA2) composed of a major tabular sandstone beds that occur laterally as a confined bodies exceeding 2.0–15.0 m in thickness with minor coarse sub-facies. The composed sandbodies; crudely stratified sandstone sub-facies (Se), massive sandstone sub-facies (Sm) and minor planar cross-bedded sandstone sub-facies (Sp) and minor horizontally stratified sandstone sub-facies (Sh) are interpreted as braided fluvial channel as suggested by Miall (1996). OFA2 may also be interpreted to represent channelized fluvial flow changing from gravel-dominated braided rivers (in proximal settings) to sandy braided river further away according to Blum and Aslan (2006). The morphology of the channel varies from ~20 to 50 meters thick with 100 meters wide bodies of tabular sandstone. The fining upward sequences dominate the OFA2 and it commonly overlies OFA1 as it is clearly represented at Shonga and Rabba (Figure 4aii). Minor to moderate bioturbation is typically observed near the top of major tabular sandstones.

Outcrop Facies Association 3 (OFA-3)

The outcrop facies association 3 (OFA3) composed basically of horizontally stratified sandstone sub-facies (Sh), planar cross-bedded sandstone sub-facies (Sp), crudely stratified sandstone sub-facies (Se), massive sandstone sub-facies (Sm) with minor crudely bedded conglomerate (Gh) sub-facies. The interrelationships of the sub-facies that make this association usually form a lenticular sandbodies dominantly of meandering channels (Figure 4bi). The morphology of the channelized sandstone bodies is highly variable; 10 to 20 meters thick, ~10 meters wide. The nature of the channels, common sedimentary structures (planar, horizontal and lamination) and the fining upwards sequences of the OFA3 are consistent with fluvial sedimentation especially

in a meandering settings according to Miall (1996) and Blum and Aslan (2006). OFA3 are well represented in the following localities; Shonga, Lafiagi, Kajita and Bida.

Outcrop Facies Association 4 (OFA4)

The outcrop facies association 4 (OFA4) is a minor body that shows the interrelationships of planar cross-bedded sandstone sub-facies (Sp), rippled laminated sandstone sub-facies (Sr), finely laminated mudstone (Fl) sub-facies with minor crudely stratified sandstone sub-facies (Se) which occurs as a sheet-like sandstone bodies or as thin restricted channels (Figure 4bii). The morphology of these sandstone bodies ranges between 5 to 20 meters thick, ~30 meters wide. Presence of reactivation surface, foreset of overtuned cross stratified, bi-directional wavy structure and burrowing of Thallasanoides, biotubation and clay drapes in this facies association suggest a tidal influence. The deposit is interpreted to be formed from upper regime laminar flow with an unconfined sheet-flow. The typical lithostratigraphic sections that exhibited OFA4 were observed at Manigi, Rabba, Enagi, Kutigi, Lafiagi and Wushishi.

Outcrop Facies Association 5 (OFA5)

The outcrop facies association 5 (OFA5) composed basically the fine sub-facies; finely laminated mudstone (Fl) sub-facies and massive mudstone sub-facies (Fm) with minor horizontally stratified sandstone sub-facies (Sh). The thickness of individual OFA5 bands can be tens of meters thick and 200m wide with erosional contact usually below or on top. The OFA5 is interpreted to represent an overbank deposits with evidence of an extensive sheet like splays which may occur during large flood occurrences distributing water and sediment across the splay (Smith *et al.,* 1989; Rhee *et al.,* 1993), and whitish to brownish variegated band characteristics. Lithological exposures of OFA5 which are typical of crevasse splay/floodplain overbank fines are commonly found at Enagi, Kutigi, Rafingora, Manigi, Tanagi and Maraba.

Architectural Elements and Sand Body Geometry

Discussions here centers on the architectural elements and body geometry analysis of the sandstone body observed within the study area using the bedform composition, internal sequence and external geometry of grouped facies association. Following, general classification scheme of Miall (1978a, 1978b, 1988), six architectural elements which were identified within the study area; gravel bar and bedforms (GB), sandy bedforms (SB), laminated sand sheet (LS), lateral accretion (LA), overbank or floodplain (OF) and channel (CH).

Gravel bars and bedforms (GB)

The Gravel bars and bed forms (GB) element is essentially made-up of vertically stacked layers of alluvial channels (intraformational conglomerates) and the braided fluvial channels (Tabular sandstone) elements (Figure 5ai). GB record either migrating channel bedloads comprising of coarse-grained or braided fluvial channels sediments basically of OFA1 and OFA2 that are interpreted to have been brought by higher river flow. Where GB occurs, it usually has sharp erosional bases and often erodes sand bedforms and channels which indicate a sudden increase in the velocity of the depositional current. The thicknesses of the gravel bars and bedforms are up to 10.0 m with a flat based and top gravel bar and the geometry formed is a lobate type.

Sandy Bedforms (SB) Elements

Sandy Bedforms (SB) is a tabular and sheet-like body of sand bed deposits comprising basically of OFA2, OFA3 and OFA4 (Figure 5aii and 5b). Thickness may range from 10.0 to 20.0 m thick and about 50.0 m wide. The SB architectural element characterizes a point bar and tidal channels deposit as it shows a fining-up section vertical relationship. The point bar and tidally influenced sediments in SB are suggested to be developed by the erosion of the bank and later accompanied by deposition on the opposite side of the channel where the flow is sluggish and the bedload can no longer be carried. They appear as sheet-like and occasionally ribbon type geometry and were dominated in the central and northern parts of the study area.

Lateral Accretion Element (LA)

The Lateral Accretion Element (LA) is characterized by 1.0 to 2.0 m thick and 10.0 m wide units of tabular and lenticular bodies and minor tidal channel sandstones which are dominated by packages of OFA2, OFA3 and OFA5 (Figure 5bi and 5bii). The LA element consists of different smaller-scale elements that represent components of braided fluvial, meandering channels and minor fluvial overbank in which most of these sediments were suggested to have carried onto the floodplain by suspended load that was mainly clay- and silt-sized debris but may include fine sand if the flow is rapid enough to carry sand in suspension according to Fielding and Webb (1996). The geometry of LA formed a wedge and ribbon type which typically contains fining-upward successions.

Laminated Sand Sheet Element (LS)

The laminated sand sheet element (LS) occurred and usually comprises of association of major lenticular sandstone and fluvial overbank/floodplain with basically OFA4 and OFA5 (Figure 5bii). This element with composition of laterally continuous sediments for up to 15.0 m thick occurred mainly as a sheet shaped geometry and fine-grained lithology suggests a bar-top to bar-flank sand sheet deposit.

Overbank or Floodplain Element (OF)

The overbank or floodplain architectural (OF) element composed predominantly vertical aggradations of outcrop

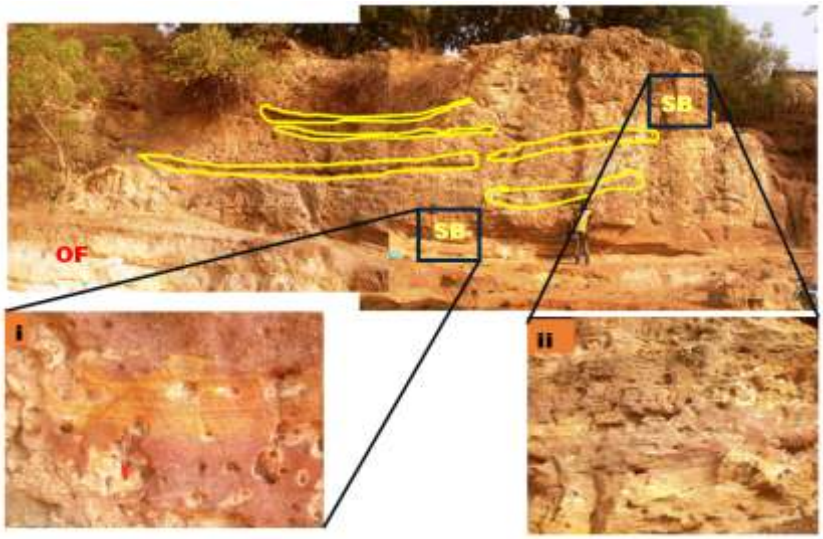


Figure 5a: (iii) An outcrop showing a typical example of Sandy Bedform (SB) and minor Overbank Fines (OF) Architectural Elements well preserved at Rabba (Longitude: 005°01.691'E; Latitude: 09°12.538N).

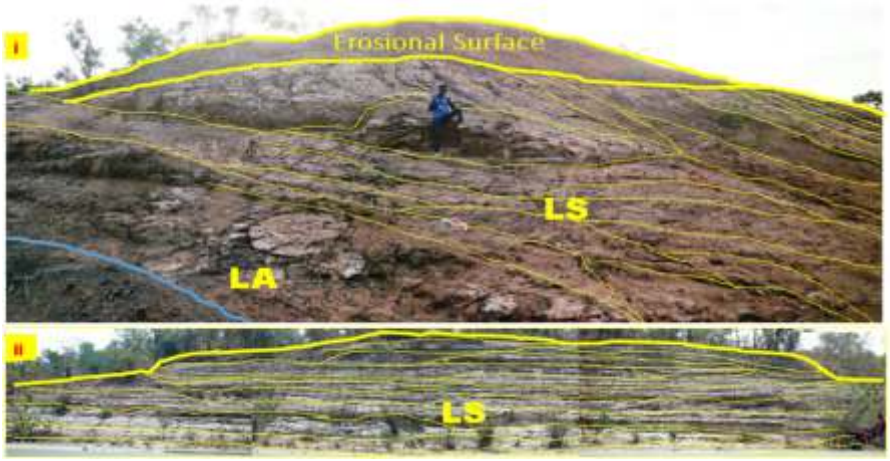


Figure 5b: Panoramic View of an outcrop showing a typical example of; (a) Lateral Accretion Element (LA) preserved at Bida (ii) Laminated Sand Sheet Element (LS) preserved at Manigi, Tanagi and Rafingora (Longitude: 005°43.798' E, Latitude: 09°55.342' N; Longitude: 005°43.799' E, Latitude: 09°55.344' N; Longitude: 005°32.277' E; Latitude: 09°46.599' N).

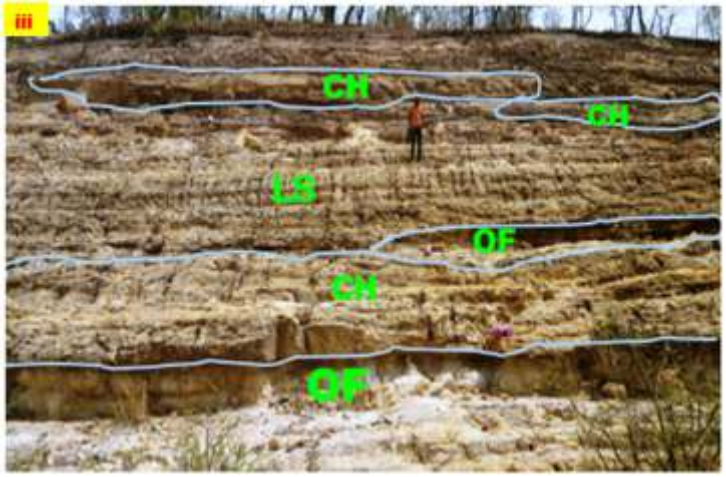


Figure 5b: An outcrop showing a typical example of a Channel Element (CH), Laminated Sand Sheet (LS) and Overbank Fines (OF) preserved at Rafingora (Longitude: 005°43.799' E; Latitude: 09°55.344').

facies association 5 (OFA5) showing thin lenses or laminae of finer sub-facies (Figure 5biii). OF element can have lateral continuous composition of up to 30.0 m thick and usually occurred mainly as normal graded, well preserved beds with evidence of less energy but high sinuosity. Generally, this element is characterized by interbeds and intercalations of finer sub-facies having basically a sheet-like shape, and in other few places as ribbon and wedge geometry.

Channels Elements (CH)

The channel elements (CH) are composed of major tabular sandstone bodies which are dominated in braided fluvial channels with minor intraformational conglomerates formed within the channel lags. The deposits of CH architectural element are usually characterized by mass flow and bedload that occur mainly at high flow stages when the bars are submerged in water. The CH elements often erode sand bedforms, frequently associated with other elements (Figure 5biii) where the total sediments fill may show several episodes of erosion and refilling. The geometry form of CH is a Lobate and Sheet types.

Paleocurrent

Palaeocurrent data were obtained from planar lamination, cross-bedding and clast imbrications (Figure 3a) within the study area for the determination of the sediment's source area and their paleoflow directions. A Window based Rose program was used for the plotting of paleocurrent measurements (Table 3). The plots indicate mostly unidirectional with minor bi-directional northeastern and northwestern paleocurrent directions (Figure 6a). This indicates major source areas were on the southwestern and southeastern directions respectively (Figure 6b).

GEOCHEMISTRY

Major Elements

Fifty (50) rock samples were selected from twelve (12) locaties for determination of major elemental composition using X-ray fluorescence methods. Result shows that SiO_2 is the dominating element while Al_2O_3, Na_2O, K_2O, Fe_2O_3 and MnO are generally comparably less except in few samples (Table 4a). The result also shows that SiO_2 contents are comparatively higher than the values of average Upper Continental Crust (UCC) after McLennan (1989) and Post-Archean Australian Shale (PAAS) after McLennan (2001) sediments while other major elements are relatively lower compared with the standards. Al_2O_3, Na_2O, K_2O, FeO and MgO are variable much lower than UCC in almost all samples.

Trace and Rare Erath Elements

Trace and rare earth elements results of the analyzed samples are presented in table 4b. Also, the rare earth elements chondrite normalized spider pattern diagram relative to the Post Archean Australian Shale (PAAS) after McLennan (2001) and Upper Continental Crust (UCC) after McLennan (1989) average values is presented in table 4c.

Zircon Morpho-Typology

Zircon is a common accessory mineral in igneous rocks (Heaman et al., 1990; Deer *et al.,* 1991; Hoskin and Schaltegger, 2003) and due to its chemical and physical durability, very useful to unravel the formation history of magmatic rocks (Corfu *et al.,* 2003). Zircon typology study is extremely valuable to identify the different rock types present in the source region (Dabard et al., 1996). Systematic zircon typology examination has led to the establishment of the widely used "Pupin diagram" (Figure 7), in which zircon crystals are classified according to the relative development of the {100}vs. {110}prismatic forms and the {211}vs. {101}pyramidal crystal forms (Pupin, 1980). The main types show 0, 1 or 2 prisms, i.e. 100 or 110 in combination with either one of the three pyramids 101, 211 or 301, or 101 + 211 arrangement to provides a better visualization of the zircon typology grid.
In this study, detrital zircon populations from two lithological sections; Agbonna and Doko ridges which belong to Enagi and Bida formations respectively were analyzed for morpho-typological (internal and external) characteristics. According to Schermaier et al. (1992), Benisek and Finger (1993), Sturm (1999), Belousova et al. (2006) and Köksal et al. (2008), the study is based upon the relative abundance of prisms and pyramids to systematically investigate zircon habits and their relation to petrogenesis. This will help provide an overview of the textural relations and their links to particular rock forming processes in view to the provenance deductions. Generally, the BSE–CL images employed in this zircon study recognized distinctly two main dominant zircon sub-populations and their morphological types.

INTERPRETATION AND DISCUSSIONS

The field observations and deductions from facies analysis and interpretations of geochemical data were synthesized together with the detrital zircon grains shape-related attributes in an attempt to discuss and constrain the sedimentation history and provenance of the sedimentary rocks in northern Bida Basin.

Facies: Gross Model and Provenance

Facies descriptions of the sedimentary exposures and the lithostratigraphic correlations across the study area have indicated a gross fluvial depositional processes and facies assemblage with occasional shallow marine tendency. The facies analysis shows that coarser sub-facies that signify high velocity/energy deposit dominate the eastern, southeastern and southwestern parts of the study area. The architectural-element analysis shows that these parts

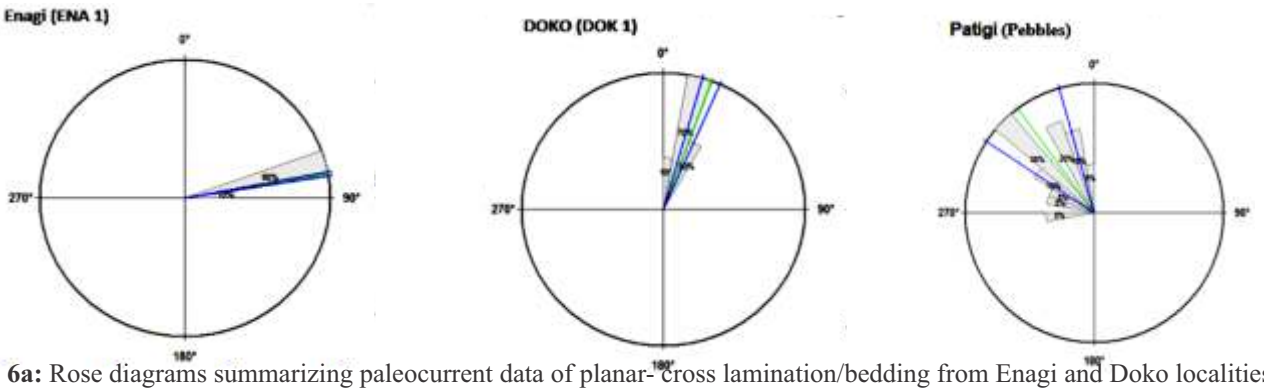


Figure 6a: Rose diagrams summarizing paleocurrent data of planar- cross lamination/bedding from Enagi and Doko localities within study area (i) The imbricated pebbles from the clast-supported, massive conglomerate (Gcm) and matrix-supported, massive conglomerate (Gmm) sub-facies preserved at Harmattan Patigi University site, Patigi (Longitude: 08°42'53.5"N; Latitude: 005°46'55.7"E), (ii) Rose diagram summarizing paleocurrent data of the clast imbrications in 3ai.

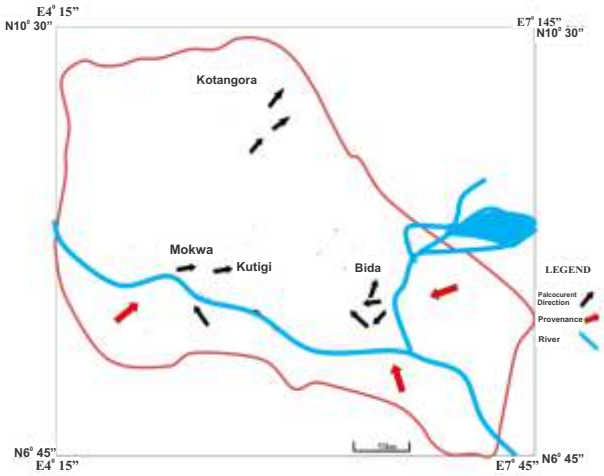


Figure 6b: Paleocurrent map of the study area.

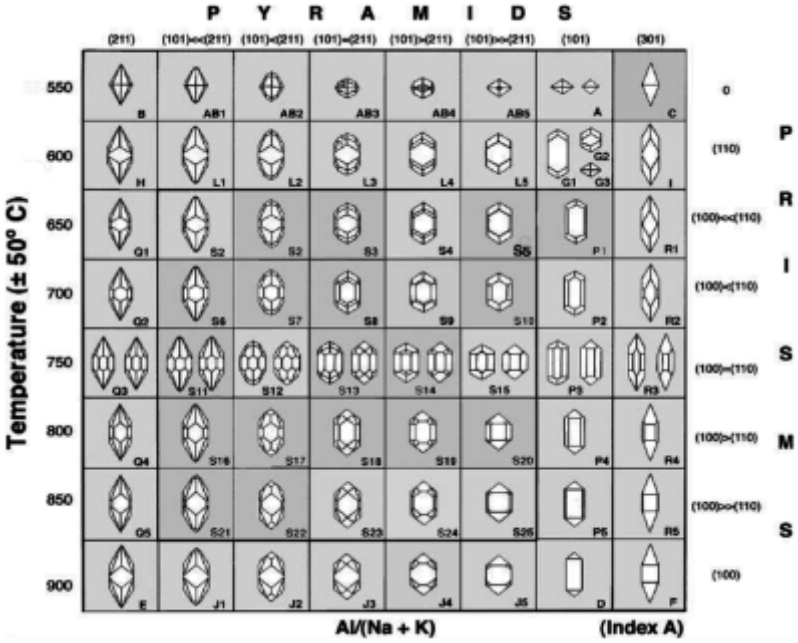


Figure 7: Zircon typological classification and corresponding geothermometric scale proposed by Pupin (1980).

comprise gravel bars and bedforms (GB) and channels (CH) with minor SB elements. According to Miall (1996), dominance of GB, CH and SB elements in sand dominated fluvial systems points to a low-sinuosity, high energy, braided river (proximal). This area therefore, represents a proximal depositional style within the source area that is probably tectonically controlled.

There was a record of lateral facies changes from the southeastern and southwestern towards the central and then to northern parts of the study area as the channel sandstones of higher energy, low sinuosity passes and changes to a braided river of less energy but higher sinuosity facies. The sandy bedforms (SB), lateral accretion (LA) and minor laminated sand sheet (LS) are the dominating elements within this part of the study area. At the northern part, the finer sub-facies characterized by laminated sand sheet (LS) and overbank fines (OF) with minor channel elements bodies predominates. Generally, the preserved sedimentary record within the study area as shown gradual transition of lithofacies depositional styles from low sinuosity, high energy, braided river (proximal) to the low energy, high-sinuosity braided river (distal) also suggests likely combinations of autocyclic and allocyclic processes as the controlling mechanisms on the sediments architecture within northern Bida Basin.

The analysis of imbricated pebbles at Patigi and interpretation of paleocurrent data reveal paleo-flow direction towards north-eastern and eastern directions with minor north-western directions indicating main source areas were on the south-western directions. Also, the tangential and dip orientation of the pebbles (18-44°W) reveals deposition by river system draining mostly from southeastern and eastern part of the northern Bida Basin implying relatively low channel sinuosity of the sediment contribution of Bida Formation from the source area.

Geochemistry: Provenance and Paleotectonics

Sandstone provenance studies are based on the assumptions that different tectonic settings contain specific compositional ranges (Dickinson and Suczek, 1979, Dickinson *et al.,* 1983; Dickinson, 1985). Crook (1974) was the first to use the framework mineral composition to identify the tectonic settings of sandstones, and other researchers have since used this scheme with modifications (e.g., Dickinson and Suczek, 1979; Dickinson *et al.,* 1883; Dickinson, 1985). Major element discrimination diagrams of Roser and Korsch (1986 & 1988) and Bhatia (1983) can also be employed to further differentiate depositional tectonic settings of sedimentary basins.

Applications of major oxides ratios; SiO_2/Al_2O_3, Al_2O_3/SiO_2, Al_2O_3/TiO_2, K_2O/Na_2O, Na_2O/K_2O, Fe_2O_3+MgO have been employed in several published research as a provenance indicator (e.g. Bock *et al.,* 1998; Gotze, 1998; Rahman and Suzuki, 2007) and in tectonic setting evaluation (e.g. Potter, 1978; Schwab, 1978; Holland, 1984; Condie and Wronkiewicz, 1990). The ratios were also employed in this study and their calculated ratios are presented in table 4a. All the studied sandstone generally show high SiO_2/Al_2O_3 values which thus reflects abundance of silica content with relatively high Al_2O_3/TiO_2 ratio which may indicate detrital material derivation from a continental source as stated by Fyffe and Pickerill (1993). Also, slightly high K_2O/Na_2O ratio may indicate presence of K-bearing minerals such as K-feldspar, muscovite and biotite according to McLennan et al. (1983) and Osae *et al.,* (2000).

The abundance of trace elements geochemistry; Cr, Ni, Zr and Hf in siliciclastics can be considered as a proxy in provenance studies. Wrafter and Graham (1989), Graver et al. (1996) and Amstrong-Altrin et al. (2004) concluded that a high content of Cr and Ni is predominantly found in sediments derived from ultramafic rocks, whereas a low concentration of Cr and Ni indicates a felsic provenance. Garver et al. (1996) has also shown that elevated Cr (Cr>150) and Ni (Ni>100) abundances are indicative of ultramafic rocks in the source region. In this study, the result of low Cr and Ni concentrations (Table 4b) may indicate felsic rocks in the source region. Higher concentration of Zr and Hf (Table 4b) which is an indication of zircon enrichment is also associated with felsic igneous rocks. The ratios between relatively immobile trace elements such as La/Sc, Th/Sc, Cr/Th and Th/Co are also considered by Taylor and McLennan (1985), Wronkiewicz and Condie (1990), and Cullers (1994 and 2000) as good source rocks indicators. Cullers and Podkovyrov (2000) and Armstrong-Altrin et al. (2004) concluded that La/Sc and Th/Sc ratios of sediments derived from felsic rocks are always higher than those of sediments derived from mafic rocks. In this study, ratios of the analyzed samples (Table 4b) compared relatively well with the ratios of sediments derived from the PAAS and UCC (Table 4c). This, thus, clearly indicate felsic source for the studied sandstones.

Discrimant plots were also employed to discriminate the sediment's source area. The binary plot of TiO_2 versus Zr (ppm) after Hayashi *et al.,* (1997) shows that the studied sandstones exhibit a predominantly felsic lithology of the source area (Figure 8a). The relationship between the composition of the source rock and sedimentary processes were also analyzed by a Zr/Sc versus Th/Sc bivariate plot after McLennan et al. (1993) to evaluate the Zr enrichment during sediment sorting. On this plot (Figure 8i), the samples plot along the zircon concentration trend, indicating zircon enrichment during sorting and recycling processes.

It was concluded by Cullers and Graf (1983), McLennan et al. (1993) and Cullers (1994, 2000) that felsic rocks

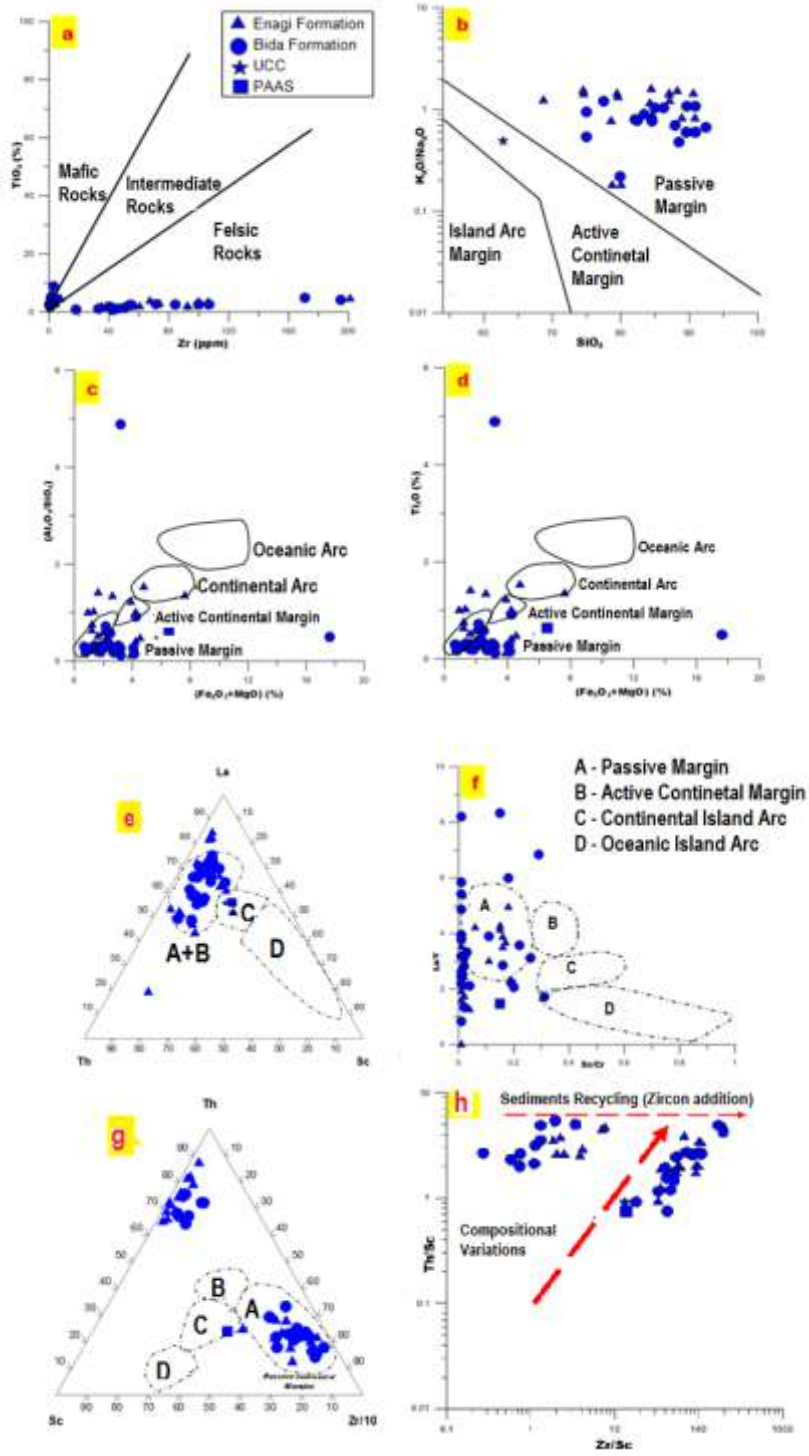


Figure 8a: Provenance bivariate discrimination plot of TiO_2 versus Zr (ppm) after Hayashi et al. (1997) showing that Northern Bida Basin sandstones were derived from felsic Igneous Rocks.

Figure 8: Paleotectonic bivariate discrimination plots; (b) log(K_2O/Na_2O) versus SiO_2 (%) after Roser and Korsch (1986), (c) (Al_2O_3/SiO_2) versus (Fe_2O_3+MgO) after Bhatia (1983), (d) TiO_2 versus (Fe_2O_3+MgO) after Bhatia (1983), (e) La-Th-Sc after Bhatia and Crook (1986), (f) La/Y versus Sc/Cr after Bhatia and Crook (1986) and (g) Th-Sc-Zr/10 after Bhatia and Crook (1986) showing Passive Margin for the investigated Bida Basin sandstones.

Figure 8h: Bivariate of Th/Sc versus Zr/Sc after McLennan et al. (1993) showing a trend to high Zr/Sc-ratios, indicating zircon addition to the sediment and therefore suggesting a recycling of an older sourced rock for the investigated Northern Bida Basin sandstone.

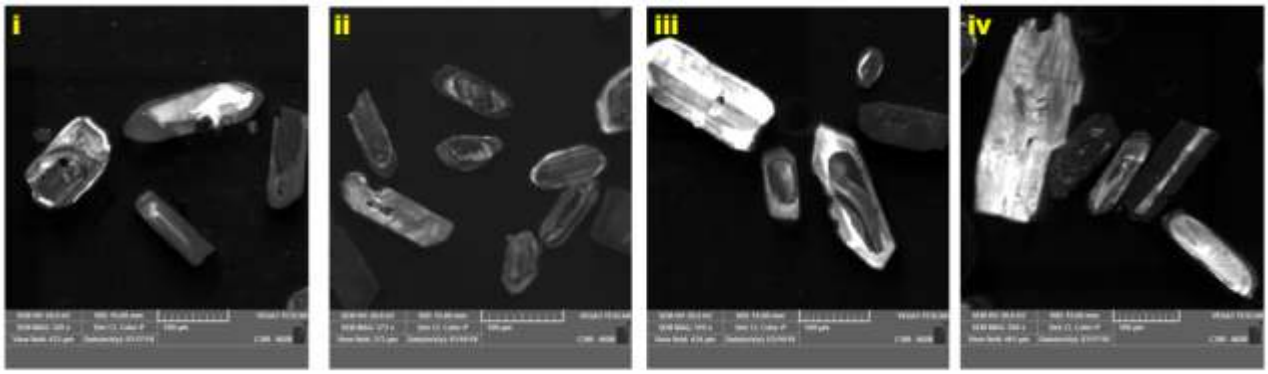


Figure 9a: Cathodoluminisence images showing representative assemblage of detrital zircon populations from Agbonna Ridge exposed at Agbonna Ridge, Share (Enagi Formation), Northern Bida Basin.

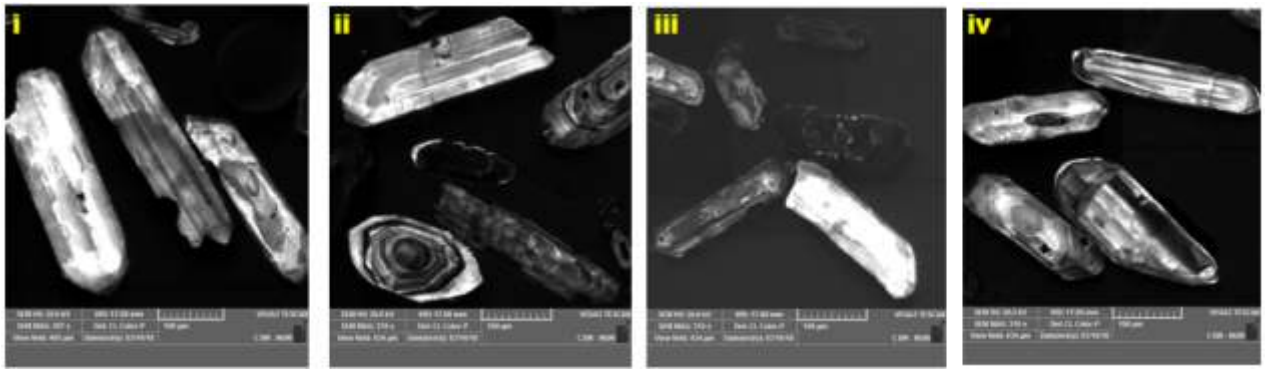


Figure 9b: Cathodoluminisence images showing representative assemblage of detrital zircon populations from Doko Ridge, Doko (Bida Formation), Northern Bida Basin.

normally contain higher LREE, lower HREE and higher LREE/HREE ratios with negative Eu anomalies, whereas mafic rocks generally contain lower LREE, higher HREE and lower LREE/HREE ratios with positive Europium anomalies (Eu*). In this study, the analyzed samples show results (Table4c) which are exclusively indicative of felsic composition in the source area. Application of the REE patterns (chondrite-normalized) has also been metoned by Taylor and McLennan (1985) to be very important in distinguishing between felsic and mafic source rock lithologies of sedimentary rocks. The chondrite-normalized pattern of the studied sandstones show LREE enrichment, almost flat HREE and negative Eu anomalies which is similar to PAAS and this suggests a felsic source rocks for the Bida Basin sediments.

Application of geochemical (major and trace elements) data of sedimentary rocks to generate tectonic discrimination diagrams (binary and ternary) has been extensively employed by Bhatia (1983, 1984 and 1985), Roser and Korsch (1986 and 1988), McLennan and Taylor (1991) and many other researchers. Those diagrams are also employed in this study to discriminate the paleotectonics of the Bida Basin. For example, the discriminant binary plots of Roser and Korsch (1986) based on $\log(K_2O/Na_2O)$ versus $SiO_2\%$, Al_2O_3/SiO_2 versus Fe_2O_3+MgO after Bhatia (1983), TiO_2 versus (Fe_2O_3+MgO) after Bhatia (1983), La/Y versus Sc/Cr after Bhatia and Crook (1986) as well as the ternary plots of $SiO_2/20$-(K_2O+Na_2O)-(TiO_2+Fe_2O_3+MgO) after Kroonenberg (1994), La-Th-Sc after Bhatia and Crook (1986) and Th-Sc-Zr/10 after Bhatia and Crook (1986) presented in figures 8a-8h the shows that the studied sandstone were plotted within passive continental depositional setting.

Zircon: Regional sources and Provenance

Agbonna Ridge (Enagi Formation)

The studied zircons were selected from Agbonna ridge, Share; AGB-1B (lower), AGB-1G (middle) and AGB-1Q (upper) parts of the section. They have higher population of relatively smaller, short and quite sharp euhedral crystals (Figure 9a) but fewer larger varieties. Generally, the zircon grain ranges from equant to prismatic and exhibit crystal outline, nebulitic with dark boundaries. Concentric type zoning are common features while few with xenocrystic cores were also observed. Some grains show an inherited core with rounded or subrounded outlines (Figure 8ai & iii) while some are characterized by an external well-developed magmatic oscillatory zoning whereas, the lamellar varieties show homogeneous crystals devoid of cores (Figure 9aii).

The internal morphological study indicated two type of

zircon sub-populations; Type 1 zircons has an inner zone with equal development of well-developed {110} prism and two pyramids, {101}and {211} of Pupin's typological classification. The dominance sub-population belongs to subtypes S9, S10 and P2 (Figure 9ai, ii & iv). Type 2 zircons show minor sub-populations record presence of {110} prism form and {101} pyramid of Pupin's typological classification one well developed with subtypes P1 and/or P3. These morphological types, according to Pupin's scale, are common in crustal or mainly crustal origin.

Doko Ridge (Bida Formation)

The studied zircons were selected from 3 sampled beds of the Doko ridge; DOK-1F, DOK-1N and DOK-1Y which are from the lower, middle and upper parts of the outcrop section. The population has relatively higher lager and mostly angular fragments types (Figure 9b). The zircon morphotypes indicate complexly zoned core, surrounded by a rim of euhedral regular fine oscillatory structures with patchy patterns (Figure 9bii & iv). Other observed varieties includes; prismatic (long) and lamellar with latter having very homogeneous crystals devoid of cores and showing dominantly oscillatory internal structures.

The internal morphological study of zircon indicated two zircon sub-populations; Type 1 zircon sub-populations typical have a well-developed prism {100} and {110}and pyramid {101}forms with the predominant subtypes P1, P2, P3, P4 and P5 of Pupin's typological classification (Figure 9bi, iii & iv). Type 2 zircon crystals have a well-defined prism {110} and pyramid {101} with less predominant subtypes S9 and S10 (Figure 8aiii). The zircon population here characterizes magmatic crystallization rocks.

CONCLUSIONS

This study focused on the provenance determination of the Campanian-Maastrichtian sandstone in the northern part of Bida Basin using facies analysis, whole-rock geochemistry and detrital zircon typo-morphological studies. Sedimentological studies identified ten sub-facies, five facies associations, six architectural elements and four sandbody geometry that occurred in a predictable order within the individual fining and coarsening-upward cycles and interpreted as fluvial to shallow marine environments. The coarse (conglomerates and sandstones) sub-facies which are most frequent in the eastern and south-eastern part of the study area is interpreted as high energy braided system with low sinuosity channels and are typical of the Bida Formation. The lateral facies changes were recorded in the central to northern parts of the study area as the channel sandstones of higher energy, low sinuosity passes to braided river of less energy but higher sinuosity (overbank fines of claystone, siltstone and silty-claystone facies). The paleocurrent data from the pebble imbrications and important sedimentary structures indicate a major flow towards northeastern and eastern directions with minor northwestern directions.

Geochemical proxies (Al_2O_3/TiO_2, SiO_2/Al_2O_3, K_2O/Al_2O_3, La/Th, La/Co, Th/Co, La/Sc, Cr/Th, Zr/Nb and Zr/Th), a light rare earth elements (LREE) enrichment, flat heavy rare earth elements (HREE), low LREE/HREE and negative Eu anomalies revealed that the studied sandstones were mainly derived from felsic source rocks. The discriminant diagrams (K_2O/Na_2O versus SiO_2%, La-Th-Sc, La-Th-Zr/10 and La/Y versus Sc/Cr) illustrate that thet were deposited in an evolving passive continental margin setting during the Campanian-Maastrichtian period of Cretaceous. Similarity of REE patterns to the published PAAS and UCC also supported the above deductions. Moreover, a binary plot of Th/Sc and Zr/Sc as well as Zr/Hf ratios show considerable enrichment of zircon, a finding that indicates recycling in the source area.

There is a remarkable morpho-typology difference between zircons from Share which belong to Enagi Formation and that of Doko that is part of Bida Formation; zircon samples from Share have predominance of short and acicular, nebulitic zircon varieties whereas Doko samples recorded dominance of complexly zoned core, xenocrystic, oscillatory, prismatic zircon types. The prismatic zircon types with a well-developed oscillatory zoning observed in Bida Formation is typical of magmatic crystallization whereas populations of short and acicular zircon varieties in Enagi Formation characterizes preservation of crustal rocks. These differences in zircon sub-populations can be interpreted as a provenance signal. This may suggest a sediment supply probably from two main sources or a possible mixing from two igneous source materials during depositional history.

REFERENCES CITED

Adeleye, D.R. and Desauvagie, T.F.J. (1972): Stratigraphy of the Niger Embayment near Bida, Nigeria. In: T. F. J. Dessauvagie and A. J. Whiteman (eds), African Geology, University of Ibadan Press. p. 181-186.

Akande, S.O., Ojo, O.J. and Ladipo, K. (2005): Upper Cretaceous sequences in the southern Bida Basin, Nigeria; A Field Guidebook, Mosuro Publishers, Ibadan, 60pp.

Armstrong-Altrin, J.S., Lee, Y.I., Verma, S.P. and Ramasamy, S. (2004): Geochemistry of sandstones from the upper Miocene Kudankulam Formation, southern India: Implications for provenance, weathering, and tectonic setting. Journal of Sedimentary Research, 74, 285-297.

Belousova, E.A., Griffin, W.L. and Pearson, N.J. (1998): Trace element composition and cathodoluminescence properties of southern African kimberlitic zircons. Mineral Magazine, 62, 355-366.

Benisek, A. and Finger, F. (1993): Factors controlling the development of prism faces in granite zircons: A microprobe study.

Contributions to Mineralogy and Petrology, 114, 441-451.

Bhatia, M.R. (1983): Plate tectonics and geochemical composition of sandstones. The Journal of Geology, 91, 611-627.

Bhatia, M.R. (1984): Rare earth element geochemistry of Australian Paleozoic graywackes and mudrocks: Provenance and tectonic control. Sedimentary Geology, 45, 97-113.

Bhatia, M.R. (1985): Rare earth element geochemistry of Australian Paleozoic graywackes and mudrocks: Provenance and tectonic control. Sedimentary Geology, 45, 97–113.

Bhatia, M.R. and Crook, K.A.W. (1986): Trace element characteristics of graywackes and tectonic setting discrimination of sedimentary basins. Contributions to Mineralogy and Petrology 92, 181–193.

Blum, M.D. and Aslan, A. (2006): Signatures of climate vs. sea-level change within incised valley-fill successions: Quaternary examples from the Texas Gulf Coast: Sedimentary Geology, 190, 177–211.

Bock, B., McLennan, S.M. and Hanson, G.N. (1998): Geochemistry and provenance of the Middle Ordovician Austin Glen Member (Normanskill Formation) and the Taconian Orogeny in New England. Journal of Sedimentology, 45, 635–655.

Braide, S.P. (1992): Syntectonic fluvial sedimentation in the central Bida Basin. Journal of Mining and Geology, 28, 55-64.

Cant, D.J. (1982): Fluvial facies models and their significance. In P.A. Scholle and D. R. Spearing (eds). Sandstone Depositional Environments, AAPG Memoir, 115-137.

Collinson, J.D. (1970): Bedformsof the Tana River.Norway. Geografiska Annaler 53a, 31–56.

Collinson, J.D. (1995): Alluvial sediments. In: Sedimentary Environments: Processes, Facies and Stratigraphy (Ed. Reading, H.G.). Blackwell Science, Oxford, p. 37–82.

Collinson, J.D. (1996): Alluvial sediments. In: Reading, H.G. (ed.). Sedimentary Environments: Processes, Facies and Stratigraphy. London, Blackswell Scientific Publications. pp. 37-82.

Condie, K.C. and Wronkiewicz, D.J. (1990): A new look at the Archean-Proterozoic boundary: Sediments and the tectonic setting constraint. In: S.M. Naqvi (Editor), Precambrian Continental Crust and Its Economic Resources. Elsevier, Amsterdam, 61-84.

Corfu, F., Hanchar, J.M. and Kinny, P. (2003): Atlas of zircon textures. Reviews in Mineralogy and Geochemistry, 53, 468–500.

Crook, K.A.W. (1974): Lithogenesis and geotectonics: the significance of compositional variation in flysch arenites (graywackes). In: Dott Jr., R.H., Shaver, R.H. (Eds.), Modern and Ancient Geosynclinal Sedimentation, SEPM Special Publication, 19, 304–310.

Cullers, R.L. (1994): The controls on the major and trace element evolution of shales, siltstones and sandstones of Ordovician to Tertiary age in the Wet Mountain region, Colorado, U.S.A. Chemical Geology, 123(1-4), 107-131.

Cullers, R.L. (2000): The geochemistry of shales, siltstones and sandstones of Pennsylvanian-Permianage, Colorado, U.S.A.: implications for provenance and metamorphic studies. Lithos, 51, 181–203.

Cullers, R.L. and Graf, J. (1983): Rare earth elements in igneous rocks of the continental crust: intermediate and silicic rocks, or petrogenesis. Rare-Earth Geochemistry, Elsevier, Amsterdam, 275-312.

Cullers, R.L. and Podkovyrov, V.N. (2000): Geochemistry of the Mesoproterozoic Lakhanda shales in southeastern Yakutia, Russia: implications for mineralogical and provenance control, and recycling. Precambrian Research, 104, 77–93.

Dabard, M.P., Loi, A. and Peucat, J.J. (1996): Zircon typology combined with Sm-Nd whole-rock isotope analysis to study Brioverian sediments from the American Massif. Journal of Sedimentary Geology, 101, 243-260.

Deer, W.A., Howie, A. and Zussman, J. (1991): An Introduction to the Rock-forming Minerals. Longman, London, 528p.

Dickinson, W.R. (1985): Interpreting provenance relations from detrital modes of sandstones. In: Zuffa, G.G. (Ed.), Provenance of Arenites. NATO-ASI Series, 148. Reidel Publishing Company, Dordrecht, 333–361.

Dickinson, W.R. and Suczek, C.A. (1979): Plate tectonics and sandstone compositions. American Association of Petroleum Geologists Bulletin, 63, 2164–2182.

Dickinson, W.R., Beard, L.S., Brakenridge, G.R., Evjavec, J.L., Ferguson, R.C., Inman, K.F., Knepp, R.A., Lindberg, F.A. and Ryberg, P.T. (1983: Provenance of North American Phanerozoic sandstones in relation to tectonic setting. Geological Society of America Bulletin, 94, 222–234.

Fielding, C.R. and Webb, J.A. (1995): Facies and cyclicity of the Late Permian Bainmedart coal measures in the northern Prince Charles Mountains, MacRobertson Land, Antarctica. Sedimentology, 43, 295–322.

Fyffe, L.R. and Pickerill, R.K. (1993): Geochemistry of Upper Cambrian-Lower Ordovician black shale along a northeastern Appalachian transect. Geol. Soc. Am. Bull. 105, 896–910.

Garver, J.I., Royce, P.R. and Smick, T.A. (1996): Chromium and Nickel in Shale of the Taconic Foreland; a Case Study for the Provenance of Fine-Grained Sediments with an Ultramafic Source. Journal of Sedimentary Research, 66, 100–106.

Gotze, J. (1998): Geochemistry and provenance of the Altendorf feldspathic sandstone in the Middle Bunter of the Thuringian basin (Germany). Chemical Geology, 150, 43-61.

Hayashi, K., Fujisawa, H., Holland, H. and Ohmoto, H. (1997): Geochemistry of 1.9 Ga sedimentary rocks from northeastern Labrador, Canada. Geochimica et Cosmochimica Acta, 61(19), 4115-4137.

Heaman, L.M., Bowins, R. and Crocket, J. (1990): The chemical composition of igneous zircon suites: implications for geochemical tracer studies. Geochimica et Cosmochimica Acta, 54, 1597–1607.

Holland, H.D. (1984): The Chemical Evolution of the Atmosphere and Oceans. Princeton University Press, Princeton, NJ, 582 p.

Hoskin, P.W.O. and Schaltegger, U. (2003): The composition of zircon and igneous and metamorphic petrogenesis. Reviews in Mineralogy and Geochemistry, 53, 27–62.

Jan du Chene, J., Adegoke, O.S., Adediran, S.A. and Petters, S.W. (1979): Palynology and Foraminifera of the Lokoja Sandstone

(Maastrichtian), Bida Basin Nigeria: Revista Espanola de Micropaleontologia, 10(3), 379 –393.

Kennedy, W.Q. (1965): The influence of basement structure on the evolution of the coastal (Mesozoic and Tertiary) basins. In: Recent Basins around Africa, Proceedings of the Institute of Petroleum Geologists Society, London p. 35–47.

King, L.C. (1950): Outline and distribution of Gondwanaland. Geological Magazine, 87, 353-359.

Kogbe, C.A. (1981): Geological Interpretation of Landsat Imagery of part of Central of central Nigeria. Journal of Mining and Geology, 28, 66-69.

Köksal, S., Göncüoglu, M., Toksoy-Köksal, F., Möller, A. and Kemnitz, H. (2008): Zircon typologies and internal structures as petrogenetic indicators in contrasting granitoids types from central Anatolia, Turkey. Mineral Petrology, 93, 185–211.

Kroonenberg, S.B. (1994): Effects of Provenance, sorting and weathering on the geochemistry of fluvial sands from different tectonic and climatic environment. Proceedings of the 29th International Geological Congress, Part A, 69-81.

McLennan, S.M. (1989): Rare earth elements in sedimentary rocks; influence of provenance and sedimentary processes, In Lipin, B.R., McKay, G.A. (eds.), Geochemistry and Mineralogy of Rare Earth Elements. Reviews in Mineralogy, 21, 169-200.

McLennan, S.M. (2001): Relation between the trace element composition of sedimentary rocks and upper continental crust. Geochem. Geophys. Geosyst., 2(4), 1021.

Mclennan, S.M. and Taylor, S.R. (1991): Sedimentary rocks and crustal evolution: tectonic setting and secular trends. Journal of Geology, 99, 1-21.

McLennan, S.M., Hemming, S., McDaniel, D.K. and Hanson, G.N. (1993): Geochemical approaches to sedimentation, provenance, and tectonics. In: Johnsson, M.J., Basu, A. (Eds.), Processes Controlling the Composition of Clastic Sediments. Special Paper of Geological Society of America, 284, 21–40.

McLennan, S.M., Taylor, S.R., Eriksson, K.A. (1983): Geochemistry of Archaean shales from the Pilbara Supergroup, Western Australia. Geochim. Cosmochim. Acta, 47, 1211–1222.

Miall A.D. (1977): Fluvial Sedimentology. Canadian Society of Petroleum Geologists, Calgary, 111 pp.

Miall, A.D. (1985): Architectural-element analysis: a new method of facies analysis applied to fluvial deposits. Earth Science Reviews, 22, 261-308.

Miall, A.D. (1988): Architectural elements and bounding surfaces in fluvial deposits: anatomy of the Kagenta Formation (Lower Jurasssic), southwest Colorado. Sedimentary Geology, 55, 233-262.

Miall, A.D. (1992): Alluvial deposits. In R.G. Walker and N.P. James, eds., Facies models: response to sea level change. Geological Association of Canada, 119-142.

Miall, A.D. (1996): The Geology of Fluvial Deposits: Sedimentary Facies, Basin Analysis, and Petroleum Geology. Heidelberg, Springer Verlag Inc., 582 p.

Ojo O. J. (2012): Depositional Environments and Petrographic Characteristics of Bida Formation around Share-Pategi, Northern Bida Basin, Nigeria: Journal of Geography and Geology, 4(1), 224-241.

Ojo O.J. (2010): Occurrence of some Maastrichtian dinoflagellate cysts from the Upper Cretaceous sediments, in southeastern Bida Basin, Nigeria: Implications for age and paleoenvironments. Global Journal of Geological Sciences, 8, 217-230.

Ojo, O. J. and Akande, S. O. (2003): Facies Relationships and Depositional Environments of the Upper Cretaceous Lokoja Formation in the Bida Basin, Nigeria. Journal of Mining and Geology, 39, 39-48.

Ojo, O.J. and Akande, S.O. (2009): Sedimentology and depositional environments of the Maastrichtian Patti Formation, southeastern Bida Basin, Nigeria: Cretaceous Research, 30: 1415-1425.

Ojo, S.B. (1984): Middle Niger Basin Revisited, Magnetic constraints on gravity interpretations. Nigerian Mining and Geosciences Society Conference, Nsukka, Nigeria, Abstract vol., p. 52-53.

Ojo, S.B. and Ajakaiye, D.E. (1989): Preliminary interpretation of gravity measurement in the middle Niger Basin area, Nigeria. In; C.A. Kogbe (ed) Geology of Nigeria, 2nd Edition, Elizabeth Publishing Co., Lagos, pp. 347-358.

Olaniyan, O. and Olabaniyi, S.B. (1996): Facies analysis of the Bida Sandstone Formation around Kajita, Nupe Basin, Nigeria. Journal of African Earth Sciences, 23, 253-256.

Osae, S., Asiedu, D.K., Banoeng-Yakubo, B., Koeberl, C. and Dampare, S.B. (2006): Provenance and tectonic setting of Late Proterozoic Buem sandstones of southeastern Ghana: evidence from geochemistry and detrital modes. Journal of African Earth Sciences 44, 85–96.

Pettijohn, F.J. (1957): "Sedimentary Rocks" (2rd Ed), Harper and Bros, New York, 718p.

Potter, P.E. (1978): Petrology and chemistry of modern big river sands. Journal of Geology, 86, 423-449.

Prothero, D.R. and Schwab, F. (2004): Sedimentary Geology: An Introduction to Sedimentary Rocks and Stratigraphy (2nd Edition), New York, W, H, Freeman and Co., 557 p.

Pupin, J.P. (1980: Zircon and granite petrology. Contributions to Mineralogy and Petrology, 73, 207–220.

Rahman, M.J.J. and Suzuki, S. (2007): Composition of Neogene shales from the Surma Group, Bengal Basin, Bangladesh: implications for provenance and tectonic setting. Austrian Journal of Earth Sciences, 100, 54-64.

Rhee, C.W., Ryand. W.H. and Chough, S.K. (1993): Contrasting development patterns of crevasse channel deposits in Cretaceous alluvial successions, Korea. Sedimentary Geolology, 85, 401-410.

Roser, B.P. and Korsch, R.J. (1986): Determination of tectonic setting of sandstone-mudstone suites using SiO2 content and K2O/Na2O ratio. Journal of Geology, 94, 635–650.

Roser, B.P. and Korsch, R.J. (1988): Provenance signatures of sandstone-mudstone suites determined using discrimination function analysis of major-element data. Chemical Geology, 67, 119–139.

Schermaier, A., Haunschmid, B., Schubert, G. and Frasl, G. (1992):

Diskriminierung von S-Typ und I-Typ Graniten auf der Basis zircon typologischer Untersuchungen. Frankfurter Geowissenschaftliche Arbeiten Serie A, 149–153.

Schwab, F.L. (1978): Modern and ancient sedimentary Utah. Sedimentology, 25, 97–109.

Schwab, F.L. (1981): Evolution of the western continental margin. French-Italian Alps: sandstone mineralogy as an index of plate tectonic setting. Jour. Geol., 89, 349-368.

Schwab, F.L. (1986): Sedimentary "signatures" of foreland basin assemblages: real or counterfeit? In: Allen, P.A., and Homewood, P (Eds.) Foreland basins: Int. Assoc. Sediment. Sp. Publ., 8, 395-410.

Smith, N.D. (1970): The braided stream depositional environment: comparison of the Platte River with some Silurian clastic rocks: north-central Appalachians. Geol. Soc. Am. Bull. 81, 2993–3041.

Smith, N.D. (1972): Some sedimentological aspects of planar cross-stratification in a sandy braided river. J. Sediment. Pet. 42, 624–634.

Sturm, R. (1999): Longitudinal and cross section of zircon: a new method for theinvestigation of morphological evolutional trends. Schweiz. Mineral Petrograpic Mitt. 79, 309–315.

Taylor, S.R. and McLennan, S.M. (1985): The Continental Crust: Its Composition and Evolution. Blackwell Scientific Publications, Oxford, 312p.

Udensi, E.E. and Osasuwa, I.B. (2004): Spectra determination of depths to magnetic rocks under the Nupe Basin, Nigeria. Nigeria Association of Petroleum Explorationists Bulletin, 17, 22-37.

Walker, R.G. (1978): Facies models. Geo. Sci. Canada Rep. Ser., v. 1, p. 171–188.

Wronkiewicz, D.J. and Condie, K.C. (1990): Geochemistry and provenance of sediments from the Pongola Supergroup, South Africa: Evidence for a 3.0-Ga-old continental Craton. Geochimica et Cosmochimica Acta, 53, 1537–1549.


NIGERIAN ASSOCIATION OF
SINCE
1975
PETROLEUM EXPLORATIONISTS